THE LINEARIZED WESTERVELT–PENNES BIOHEAT SYSTEM: NUMERICAL ANALYSIS AND SIMULATION

J. A. FERREIRA, F. OLIVEIRA, AND G. PENA

ABSTRACT. In this paper we study an accurate and stable numerical method for the system of partial differential equations defined by the linearized Westervelt equation and the Pennes bioheat equation. This system was proposed in the literature to describe the high-intensity focused ultrasound (HIFU) propagation through a target tissue and the correspondent temperature evolution due to the conversion of acoustic energy into heat. In the bioheat equation, the heat source term is allowed to depend on the acoustic field through p^2, p_t^2 or on suitable time-averaged versions of these quantities. The method can be seen simultaneously as a finite difference method and as a fully discrete in space piecewise linear finite element method. We establish second order convergence in space for the discrete time derivative and for the discrete gradient of the numerical solution and first order convergence in time, including the case where the temperature equation is driven by the aforementioned heat sources. Semi-discrete and fully discrete in time and space discretizations are studied using the Bramble-Hilbert lemma to avoid the usual smoothness requirements on the solution. Simulation results illustrating the convergence estimates and the qualitative behavior of the solution of the differential problem are also included.

1. INTRODUCTION

Ultrasounds have been a staple in clinical diagnostic for decades. More recently, its mechanical and thermal effects have led to its use in several medical applications, through high intensity focused ultrasounds (HIFU), see [5, 9, 10, 30]. Therefore, accurately simulating the propagation of HIFU plays a crucial role in treatment planning. In this paper, we consider the Westervelt equation [10, 34],

$$p_{tt} = b\Delta p_t + \alpha(T)\Delta p + k(T)(p^2)_{tt} + f, \tag{1}$$

coupled with the well known Pennes bioheat equation,

$$\gamma_0 T_t + \gamma_1 T = \gamma_2 \Delta T + g, \tag{2}$$

to model a HIFU propagating through a target tissue and the corresponding temperature evolution. This system is defined in the domain $\Omega \times (0, t_f]$, where $\Omega = (0, 1)^2$ is the spatial domain and $t_f > 0$ represents the final time. The system of partial differential equations (1) and (2) is also complemented with the initial conditions

$$p(x, y, 0) = \phi(x, y), \quad p_t(x, y, 0) = \psi(x, y), \quad T(x, y, 0) = T_0(x, y), \text{ for } (x, y) \in \Omega, \tag{3}$$

and the homogeneous Dirichlet boundary conditions

$$p(x, y, t) = 0, \quad T(x, y, t) = 0, \text{ on } \Omega \times (0, t_f], \tag{4}$$

where $\partial\Omega$ denotes the boundary of Ω. In the context of equation (2), the source term g accounts for the heat generated by the conversion of acoustic energy, as well as other potential heat sources.

The coefficients and terms in these equations have distinct physical meaning. For the Westervelt equation (1), $\alpha(T) = c^2(T)$, where $c(T)$ is the temperature-dependent speed of sound in the tissue. The term $b > 0$ is the sound diffusivity. The coefficient $k(T)$ is defined as $\frac{\beta}{\rho c^2(T)}$, where ρ is the mass density and β is the nonlinearity coefficient. Finally, f represents an external source term. For the Pennes bioheat equation (2), $\gamma_0 = \rho_a C_a$, where ρ_a is the medium density and C_a is the medium specific heat capacity. The term γ_1 is given by $C_b\omega_b$, where C_b is the specific heat capacity of blood and ω_b is the volumetric perfusion rate. The coefficient γ_2 is the thermal conductivity of the medium. The source term g is expressed as $g = Q + C_b\omega_b T_a$, where T_a is the arterial blood temperature and Q is the acoustic energy absorbed by the tissue that converts to heat. The expression of the heat source Q varies in the literature but it is modeled as being directly proportional to the acoustic intensity. However, the intensity of an acoustic wave can be expressed in different ways. For example, if the phenomenon is not very oscillatory, the intensity can be taken as the instantaneous squared acoustic pressure, p^2, or pressure velocity, p_t^2, see [12, 22]. Both expressions can be seen as equivalent, in some sense, provided we scale the pressure

Key words and phrases. Westervelt equation, Pennes equation, nonuniform finite differences, convergence and stability analysis, numerical simulation.

velocity with ω^{-2}, where ω is the angular frequency, see [27]. However, if the pressure signal is highly oscillatory, like HIFU, then it is considered more appropriate to model the intensity as a time-averaged quantity. As before, two possibilities are to model the intensity as $\langle p^2 \rangle$ or $\omega^{-2} \langle p_t^2 \rangle$, where

$$\langle p^2 \rangle (x,t) = \frac{1}{t} \int_0^t p^2(x,s)\,\mathrm{d}s.$$

In [12,22], Q is unbounded as p^2 and p_t^2 increase. This behavior is not physically acceptable in practical applications. We believe that a smoother version of these functions needs to be introduced to ensure physical accuracy. Following these considerations, we will assume that Q is a Lipschitz function depending on p^2, p_t^2, $\langle p^2 \rangle$ and $\langle p_t^2 \rangle$.

Further research into this system and its variations have explored aspects of its mathematical properties and physical interpretations. For instance, the local wellposedness of the system comprising equations (1) to (4) was established in [22], while its global wellposedness and qualitative behavior were analyzed in [23]. To account for nonfickian heat transport, the authors of [1] considered a hyperbolic heat equation as a replacement for the standard Pennes equation. This nonfickian version incorporates a relaxation time parameter τ into the heat flux, $\mathbf{J}$[1], such that $\tau \frac{\partial \mathbf{J}}{\partial t} + \mathbf{J} = -k_a \nabla T$. Additionally, in [3], the authors modified the system of equations (1) and (2) by coupling it with a convection-diffusion-reaction equation for a concentration variable, where the convective velocity is dependent on the acoustic pressure. This study also addressed the wellposedness of the newly proposed system and presented a numerical method to illustrate the behavior of its solution.

The mathematical description of ultrasound propagation through a target tissue has received broad attention in the literature. For instance, a wave equation in a heterogeneous medium is considered in [20], while in [8,16] a telegraph equation in a nonhomogeneous medium is studied. A homogeneous Helmholtz equation was analyzed in [12]. To describe ultrasound propagation in a viscoelastic tissue, the authors in [29] studied a viscoelastic wave equation written in terms of particle displacement. Other references that focus more in specific applications can also be found in the literature. Without being exhaustive we mention that ultrasounds can enhance drug delivery in several medical contexts. They can be used to locally and transiently break the blood brain barrier [26,31], and the corneal barrier, increasing its permeability [28,35]. They can also break physiological cancer barriers [13,14] and assist in treating eye diseases by temporarily disrupting the corneal barrier [28,35]. Other applications of HIFU propagation has been employed in tumor ablation (see, for instance, the reviews in [9,19]) and fat reduction [21].

In the numerical analysis of this paper, we focus on a linearized version of the Westervelt equation, neglecting the nonlinear effect term $k(T)$ and taking $\alpha(T)$ as a constant, that is, we consider

$$p_{tt} + \alpha_1 p_t = \alpha_2 \Delta p + \alpha_3 \Delta p_t + f, \tag{5}$$

and

$$T_t + \gamma_1 T = \gamma_2 \Delta T + Q(p^2, p_t^2, \langle p^2 \rangle, \langle p_t^2 \rangle) + g. \tag{6}$$

subject to the same boundary conditions and initial data as previously.

In porous tissues, and as a consequence of ultrasound propagation, convective heat transport can be observed due to occurrence of cavitation - growing, oscillation and collapsing of microbubbles, see [4]. Cavitation induces phenomenon like microstreaming, microjets and shockwaves that enhance heat and mass transfer. The Pennes bioheat equation does not take into account the convective heat transport and alternative models have been proposed in the literature. For instance, in [32,33], a particular case of equation (2) is considered to describe the temperature evolution induced by HIFU with $\mathbf{v}(p) = \mathbf{u}$ where $\mathbf{u}$ is a divergence free velocity satisfying the momentum equation

$$\mathbf{u}_t + \beta_1 \mathbf{u} = +\beta_2 \nabla \cdot (\nabla \mathbf{u} + (\nabla \mathbf{u})^T) - \beta_3 \nabla p + \beta_4 (T - T_{ref})\mathbf{g} + \mathbf{F}(p).$$

Here, $(\nabla \mathbf{u})^T$ denotes the transpose of $\nabla \mathbf{u}$, $\mathbf{g}$ denotes the gravitational acceleration and $\mathbf{F}(p)$ is a source term that takes into account the conversion of the acoustic pressure energy in heat. We note that in our paper, although our main focus will deal with the system defined by equations (5) and (6), which does not explicitly include the convective term, we will make remarks along the paper on how the analysis can be carried out if such term is present. We shall assume that the convective velocity depends on ultrasound pressure and its gradient, thereby avoiding the mathematical equations for $\mathbf{u}$.

Although the numerical simulation of ultrasound propagation through a target tissue and the corresponding temperature evolution are reported in a considerable number of papers, only a few papers focus on the development of the theoretical support on the numerical methods used. Without being exhaustive, we mention [8] where a semidiscrete approximation for the acoustic pressure and temperature induced

[1]In this paper, we will use bold letters to denote vector quantities.

by a spatial discretization defined by a finite difference method (which can be seen as a fully discrete piecewise linear finite element method) is proposed. This was used to solve the telegraph equation for the ultrasound propagation coupled with a Pennes bioheat equation for the heat evolution.

The present paper addresses the lack of theoretical support for the Westervelt–Pennes system by developing a fully discrete numerical method for the linearized Westervelt–Pennes system of equations (5) and (6) with rigorous convergence analysis. Our main contributions are (i) a semidiscrete and fully discrete finite difference method, (ii) stability and error estimates for both semidiscrete and fully discrete approximations, (iii) second order in space and first order in time convergence rates under less smoothness than the classical approach and (iv) numerical simulations illustrating the theoretical convergence rates and qualitative behavior using realistic physical parameters. Compared to [8], our analysis incorporates the additional diffusion term Δp_t in the acoustic equation and the acoustic energy absorption Q in the heat equation, and extends the analysis to fully discrete schemes.

The paper is organized as follows. In Section 2 we introduce the notations and auxiliary results that will be used in the numerical analysis of the proposed method. In Section 3 we present the semidiscrete approximation for the system defined by equations (5) and (6) and establish stability and error estimates for the corresponding numerical approximations. A fully discrete method in space and time is introduced in Section 4 where we also establish stability and error estimates for the corresponding numerical approximations. Finally, in Section 5, we present some simulation results illustrating the convergence estimates and the qualitative behavior of the solution of the differential problem, using realistic parameters.

2. Notations and auxiliary results

This section lays the groundwork for our numerical analysis. We consider the domain $\Omega = (0,1)^2$ and introduce in $\overline{\Omega}$ a nonuniform grid $\overline{\Omega}_H$ in the following way. Let $H = (\mathbf{h}, \mathbf{k})$ represent the discretization parameters, where $\mathbf{h} = (h_1, \dots, h_N)$ and $\mathbf{k} = (k_1, \dots, k_M)$ are vectors with positive entries such that $\|\mathbf{h}\|_1 = \|\mathbf{k}\|_1 = 1$, where $\|\cdot\|_p$ denotes the standard vector p-norm, with $p = 1$. We define $H_{\max} = \max\{\|\mathbf{h}\|_\infty, \|\mathbf{k}\|_\infty\}$ and $H_{\min}$ with the proper adjustments. In the subsequent analysis, we will consider a sequence of such grids, where this parameter, $H_{\max}$, tends to zero.

The set of grid points, denoted by $\overline{\Omega}_H$, is defined as

$$\overline{\Omega}_H = \{(x_i, y_j) : i = 0, \dots, N, j = 0, \dots, M\},$$

where $x_0 = y_0 = 0$, and the grid point coordinates satisfy $x_i = x_{i-1} + h_i$, for $i = 1, \dots, N$, and $y_j = y_{j-1} + k_j$, for $j = 1, \dots, M$. The discrete boundary $\partial\Omega_H$ is the intersection of $\overline{\Omega}_H$ with the boundary of the continuous domain $\partial\Omega$, i.e., $\partial\Omega_H = \overline{\Omega}_H \cap \partial\Omega$. The set of interior grid points is denoted by $\Omega_H = \overline{\Omega}_H \cap \Omega$.

Remark 1. Throughout this work, we use the notation $A \lesssim B$ to indicate that $A \leq CB$ for some positive constant C independent of the discretization parameter H and time t.

2.1. Discrete space and operators.

We denote by V_H the space of grid functions defined on $\overline{\Omega}_H$. A subspace of particular interest is $V_{H,0} = \{v_H \in V_H : v_H(x,y) = 0, (x,y) \in \partial\Omega_H\}$, which consists of grid functions that are zero on the discrete boundary.

Next, we introduce several finite difference operators. The backward difference operator in the x-direction, $D_{-x} : V_H \longrightarrow V_H$, at a point (x_i, y_j), is defined by

$$D_{-x} u_H(x_i, y_j) = \frac{u_H(x_i, y_j) - u'_H(x_{i-1}, y_j)}{h_i},$$

where we assume that, if $i = 0$, then $D_{-x} u_H(x_0, y_j) = u_H(x_0, y_j)/h_1$. The second-order centered difference operator in x, $D_{2,x} : V_H \longrightarrow V_H$, is defined using D_{-x} as

$$D_{2,x} u_H(x_i, y_j) = \frac{D_{-x} u_H(x_{i+1}, y_j) - D_{-x} u_H(x_i, y_j)}{h_{i+1/2}},$$

where $h_{i+1/2} = (h_i + h_{i+1})/2$ and, at $i = N$, we simply eliminate the term $D_{-x} u_H(x_{i+1}, y_j)$ in the previous definition. The operators D_{-y} and $D_{2,y}$ are defined analogously in the y-direction, with $k_{j+1/2} = (k_j + k_{j+1})/2$. Using these, we define the discrete gradient operator $\nabla_H : V_H \longrightarrow [V_H]^2$ as $\nabla_H u_H = (D_{-x} u_H, D_{-y} u_H)$, for $u_H \in V_H$ and the discrete Laplace operator, $\Delta_H : V_H \longrightarrow V_H$, by $\Delta_H u_H = D_{2,x} u_H + D_{2,y} u_H$, for $u_H \in V_H$.

The centered difference operator in the x-direction is defined as

$$D_{c,x} u_H(x_i, y_j) = \frac{u_H(x_{i+1}, y_j) - u_H(x_{i-1}, y_j)}{h_i + h_{i+1}}.$$

The corresponding operator in the y-direction, $D_{c,y}$, is defined analogously. We denote by $\nabla_{c,H} : V_H \longrightarrow [V_H]^2$ the operator defined by $\nabla_{c,H} u_H = (D_{c,x} u_H, D_{c,y} u_H)$, for $u_H \in V_H$. Moreover, we introduce the operators $D_h, D_k : V_H \longrightarrow V_H$. For $i = 1, \ldots, N-1$ and $j = 1, \ldots, M$, D_h is defined as

$$D_h u_H(x_i, y_j) = \frac{h_i D_{-x} u_H(x_{i+1}, y_j) + h_{i+1} D_{-x} u_H(x_i, y_j)}{h_i + h_{i+1}}.$$

At the boundaries $x = x_0$ and $x = x_N$, it is defined as $D_h u_H(x_0, y_j) = D_{-x} u_H(x_1, y_j)$ and $D_h u_H(x_N, y_j) = D_{-x} u_H(x_N, y_j)$, for $j = 1, \ldots, M$. The operator D_k is defined analogously. The combined operator $D_H : V_H \longrightarrow [V_H]^2$ is given by $D_H u_H = (D_h u_H, D_k u_H)$, for $u_H \in V_H$.

Finally, we introduce the averaging operator in the x-direction as

$$M_h u_H(x_i, y_j) = \frac{u_H(x_{i-1}, y_j) + u_H(x_i, y_j)}{2}$$

where $M_h u_H(x_0, y_j) = u_H(x_0, y_j)/2$. The operator M_k is defined similarly in the y-direction. For a pair of grid functions $\mathbf{u}_H = (u_{H,1}, u_{H,2}) \in [V_H]^2$, we use the notation

$$M_H \mathbf{u}_H = (M_h u_{H,1}, M_k u_{H,2}).$$

2.2. **Discrete inner products and norms.** We now define inner products and norms on these discrete spaces. For $u_H, v_H \in V_{H,0}$, we define

$$(u_H, v_H)_H = \sum_{(x_i,y_j) \in \overline{\Omega}_H} |\square_{i,j}| u_H(x_i, y_j) v_H(x_i, y_j),$$

where $\square_{i,j} = (x_{i-1/2}, x_{i+1/2}) \times (y_{j-1/2}, y_{j+1/2}) \cap \Omega$ is a control volume around (x_i, y_j), and $|\square_{i,j}|$ denotes its area. In this definition, we assume that the midpoints $x_{i+1/2}$ are defined as

$$x_{-1/2} = x_0, \quad x_{N+1/2} = x_N, \quad x_{i+1/2} = x_i + h_{i+1}/2, \quad j = 1, \ldots, N-1$$

and $y_{j+1/2}$ is defined similarly. The norm induced by this inner product is denoted by $\|\cdot\|_H$.

For vector grid functions $\mathbf{u}_H = (u_{H,1}, u_{H,2}), \mathbf{v}_H = (v_{H,1}, v_{H,2}) \in [V_H]^2$, we define

$$(\mathbf{u}_H, \mathbf{v}_H)_+ = (u_{H,1}, v_{H,1})_{x,+} + (u_{H,2}, v_{H,2})_{y,+},$$

where each component is given by

$$(u_{H,1}, v_{H,1})_{x,+} = \sum_{i=1}^{N} \sum_{j=1}^{M-1} h_i k_{j+1/2} u_{H,1}(x_i, y_j) v_{H,1}(x_i, y_j)$$

$$(u_{H,2}, v_{H,2})_{y,+} = \sum_{i=1}^{N-1} \sum_{j=1}^{M} h_{i+1/2} k_j u_{H,2}(x_i, y_j) v_{H,2}(x_i, y_j).$$

We note that this bilinear form is an inner product in $V_{H,0}$. The corresponding norms derived from these components for functions in $V_{H,0}$ are denoted by $\|\cdot\|_{x,+}$ and $\|\cdot\|_{y,+}$. Using these, we define a discrete norm for the gradient,

$$\|\nabla_H u_H\|_+ = \left(\|D_{-x} u_H\|_{x,+}^2 + \|D_{-y} u_H\|_{y,+}^2\right)^{1/2}.$$

With this notation, we define in V_H the following discrete norm

$$\|u_H\|_{1,H} = \left(\|u_H\|_H^2 + \|\nabla_H u_H\|_+^2\right)^{1/2}.$$

It is worth observing that the norms $\|\cdot\|_H$ and $\|\cdot\|_{1,H}$ can be interpreted as discrete analogues of the standard continuous $L^2(\Omega)$ and $H^1(\Omega)$ norms, respectively. We also introduce a discrete L^4-norm for grid functions in V_H as

$$\|u_H\|_{L^4_H} = \left(\sum_{(x_i,y_j) \in \overline{\Omega}_H} |\square_{i,j}| u_H^4(x_i, y_j) \right)^{1/4}.$$

The following two results are well known for this type of finite difference operators and corresponding inner products.

Proposition 1 (Summation by parts)**.** *For $u_H, v_H \in V_{H,0}$, the following equality holds*

$$(\Delta_H u_H, v_H)_H = -(\nabla_H u_H, \nabla_H v_H)_+.$$

Proposition 2 (Discrete Poincaré-Friedrichs inequality)**.** *For all $u_H \in V_{H,0}$, we have*

$$\|u_H\|_H \leq \|\nabla_H u_H\|_+.$$

Finally, we define discrete analogues of the $W^{s,\infty}$-norm, $s = 0, 1$. For $u_H \in V_H$ and $\mathbf{u}_H = (u_{H,1}, u_{H,2}) \in [V_H]^2$, let

$$\|u_H\|_{+,x,\infty} = \max_{\substack{i=1,\dots,N\\ j=0,\dots,M}} |u_H(x_i, y_j)|, \qquad \|u_H\|_{H,\infty} = \max_{(x_i,y_j)\in\overline{\Omega}_H} |u_H(x_i, y_j)|,$$

$$\|u_H\|_{+,y,\infty} = \max_{\substack{i=0,\dots,N\\ j=1,\dots,M}} |u_H(x_i, y_j)|, \qquad \|u_H\|_{1,H,\infty} = \max\{\|u_H\|_{H,\infty}, \|\nabla_H u_H\|_{+,\infty}\},$$

$$\|\mathbf{u}_H\|_{+,\infty} = \max\{\|u_{H,1}\|_{+,x,\infty}, \|u_{H,2}\|_{+,y,\infty}\}.$$

In the upcoming analysis, we will also require the following propositions whose proof is straightforward.

Proposition 3. *For $u_H \in V_{H,0}$, it holds*

$$\|u_H\|_{H,\infty} \le \frac{1}{H_{\min}} \|u_H\|_H,$$
$$\|u_H\|_{H,\infty} \le \frac{1}{\sqrt{2}\,H_{\min}} \|\nabla_H u_H\|_+,$$
$$\|u_H\|_{1,H,\infty} \le \frac{1}{H_{\min}^2} \|\nabla_H u_H\|_+.$$

Proposition 4. *Let $\mathbf{u}_H \in [V_{H,0}]^2$ and $v_H \in V_{H,0}$. We have*

$$(\nabla_{c,H}\cdot\mathbf{u}_H, v_H)_H = -(M_H\mathbf{u}_H, \nabla_H v_H)_+.$$

Proposition 5. *If $u_H \in V_{H,0}$ then*

$$\max\{\|D_h u_H\|_{H,\infty}, \|D_k u_H\|_{H,\infty}\} \le 2\min\{\|D_{-x}u_H\|_{+,x,\infty}, \|D_{-y}u_H\|_{+,y,\infty}\}.$$

We end this subsection by stating one result that is a discrete version of Ladyzhenskaya's inequality [22, Inequality (2.8)] in $V_{H,0}$. This result is the two-dimensional counterpart of [24, Proposition A.0.4]. In order to do so, we first present an auxiliary result that is a discrete version of the Gagliardo-Nirenberg interpolation inequality applied to $V_{H,0}$ functions per line segment.

Proposition 6 (Discrete Gagliardo-Nirenberg interpolation inequality)**.** *Let $u_H \in V_{H,0}$ and $(x_i, y_j) \in \overline{\Omega}_H$. Then,*

$$\max_{i=1,\dots,N} u_H^2(x_i, y_j) \le 2\left(\sum_{i=1}^{N-1} h_{i+1/2}u_H^2(x_i, y_j)\right)^{1/2}\left(\sum_{i=1}^{N} h_i(D_{-x}u_H(x_i, y_j))^2\right)^{1/2}$$

and

$$\max_{j=1,\dots,M} u_H^2(x_i, y_j) \le 2\left(\sum_{j=1}^{M-1} k_{j+1/2}u_H^2(x_i, y_j)\right)^{1/2}\left(\sum_{j=1}^{M} k_j(D_{-y}u_H(x_i, y_j))^2\right)^{1/2}.$$

Proof. We only prove the first inequality, as the second follows similarly. For fixed j, we consider the one-dimensional grid function $v_i = u_H(x_i, y_j)$ for $i = 0, \dots, N$. Note that $v_0 = v_N = 0$ since $u_H \in V_{H,0}$.

Let m denote the index such that $|v_m| = \max_i |v_i|$. Since $v_0 = 0$ and using the Cauchy-Schwarz inequality, we can write

$$\begin{aligned} v_m^2 &= \sum_{i=1}^{m}(v_i + v_{i-1})h_i(D_{-x}v_i) \\ &\le 2\left(\sum_{i=1}^{N} \frac{h_i}{4}(v_i + v_{i-1})^2\right)^{1/2}\left(\sum_{i=1}^{N} h_i(D_{-x}v_i)^2\right)^{1/2}. \end{aligned}$$

Finally, from the identity

$$\sum_{i=1}^{N} \frac{h_i}{4}(v_i + v_{i-1})^2 = \sum_{i=1}^{N-1} h_{i+1/2}v_i^2,$$

we conclude the proof. □

Proposition 7 (Discrete Ladyzhenskaya-type inequality)**.** *For $u_H \in V_{H,0}$, we have*

$$\|u_H\|_{L_H^4}^2 \le \sqrt{2}\,\|u_H\|_H\|\nabla_H u_H\|_+. \tag{7}$$

Proof. From the definition of $\|\cdot\|_{L^4_H}$, we have

$$\|u_H\|^2_{L^4_H} = \sum_{j=1}^{M-1} k_{j+1/2}\left(\sum_{i=1}^{N-1} h_{i+1/2} u_H^2(x_i,y_j) u_H^2(x_i,y_j)\right)$$
$$\leq \underbrace{\left(\sum_{j=1}^{M-1} k_{j+1/2} \max_{i=1,\dots,N-1} u_H^2(x_i,y_j)\right)}_{A_1} \underbrace{\left(\sum_{i=1}^{N-1} h_{i+1/2} \max_{j=1,\dots,M-1} u_H^2(x_i,y_j)\right)}_{A_2}$$

Using Proposition 6 to estimate the maximum term in A_1, we obtain successively

$$A_1 \leq 2\sum_{j=1}^{M-1} k_{j+1/2}\left[\left(\sum_{i=1}^{N-1} h_{i+1/2} u_H^2(x_i,y_j)\right)^{1/2}\left(\sum_{i=1}^{N} h_i (D_{-x}u_H(x_i,y_j))^2\right)^{1/2}\right]$$
$$\leq 2\|u_H\|_H \|D_{-x}u_H\|_{x,+},$$

and similarly, for A_2,

$$A_2 \leq 2\|u_H\|_H \|D_{-y}u_H\|_{y,+}.$$

Combining these estimates, we arrive at

$$\|u_H\|^4_{L^4_H} \leq 4\|u_H\|^2_H \|D_{-x}u_H\|_{x,+}\|D_{-y}u_H\|_{y,+},$$

which leads to inequality (7). □

2.3. **Projection and restriction operators.** Let $\mathcal{T}_H$ be the admissible triangulation of Ω induced by the nonuniform rectangular grid $\overline{\Omega}_H$. Specifically, each rectangle $[x_i,x_{i+1}]\times[y_j,y_{j+1}]$ within this grid is decomposed into two triangles: one that includes the grid vertex (x_i,y_{j+1}) as its right-angle vertex, and the other that similarly includes (x_{i+1},y_j) as its right-angle vertex. Associated with the nodes of this grid $\overline{\Omega}_H$, we denote as $P_H : V_H \longrightarrow C(\overline{\Omega})$ as the standard piecewise linear interpolation operator. We further introduce the standard restriction operator $R_H : C(\overline{\Omega}) \longrightarrow \mathbb{R}$ which evaluates a function at the grid points of $\overline{\Omega}_H$ and the Clément-type projection, $\widehat{R}_H : L^1(\Omega) \longrightarrow \mathbb{R}$, as follows

$$(\widehat{R}_H g)(x_i,y_j) = \frac{1}{|\square_{i,j}|}\iint_{\square_{i,j}} g(x,y)\,\mathrm{d}x\,\mathrm{d}y,$$

for $i=1,\dots,N-1$, $j=1,\dots,M-1$.

2.4. **Functional spaces.** To simplify the presentation of the upcoming numerical methods, we consider the following notation: if $v_H : \overline{\Omega}_H \times [0,t_f] \longrightarrow \mathbb{R}$, by $v_H(t)$, $t\in[0,t_f]$, we represent the grid function $v_H(t) : \overline{\Omega}_H \longrightarrow \mathbb{R}$, defined by $v_H(t)(x_i,y_j) = v_H(x_i,y_j,t)$, $i=0,\dots,N$ and $j=0,\dots,M$. By $v_H'(t)$ we represent its time derivative. For grid functions v_H defined in others grid sets the definition is similar. Finally, given a Banach space X and $m\in\mathbb{N}$, we introduce $C^m([0,t_f];X)$ as the space of functions $v:[0,t_f]\longrightarrow X$ such that $v^{(i)} : [0,t_f] \longrightarrow X$, $i=0,\dots,m$ are continuous, imbued with the norm

$$\|v\|_{C^m([0,t_f];X)} = \max_{t\in[0,t_f]} \|v(t)\|_X.$$

Similarly, we introduce the Bochner spaces $H^i(0,t_f;X)$ $i\geq 0$.

3. Semidiscrete approximation method

The numerical method that we will study in the present paper can be seen simultaneously as a fully discrete piecewise linear finite element (FEM) method and as a finite difference method (FDM). To introduce our method as a fully discrete piecewise linear FEM, we first introduce the weak formulations of the combination of equations (1), (2), (5) and (6). On one hand, we recover the linearized case of equation (5) making $K=0$ and on the other hand, we recover the original Westervelt equation (1).

For the coupled problem, the weak formulation is: find $p\in H^2(0,t_f;L^2(\Omega))\cap H^1(0,t_f;H^1(\Omega))\cap L^2(0,t_f;H^2(\Omega)\cap H^1_0(\Omega))$ and $T\in H^1(0,t_f;L^2(\Omega))\cap L^2(0,t_f;H^1_0(\Omega))$ such that

$$\begin{aligned}(p''(t),w_1) + \alpha_1(p'(t),w_1) + \alpha_2(\nabla p(t),\nabla w_1)_{[L^2]^2} + \alpha_3(\nabla p'(t),\nabla w_1)_{[L^2]^2}\\ = K((p^2(t))'',w_1) + (f(t),w_1)\end{aligned} \tag{8}$$

and

$$\begin{aligned}(T'(t),w_2) + \gamma_1(T(t),w_2) + \gamma_2(\nabla T(t),\nabla w_2)_{[L^2]^2}\\ = (Q(p^2(t),(p')^2(t),\langle p^2\rangle(t),\langle (p')^2\rangle(t)),w_2) + (g(t),w_2),\end{aligned} \tag{9}$$

a.e. in $(0,t_f)$, for all $w_1, w_2 \in H_0^1(\Omega)$, with the initial conditions

$$\begin{cases} (p(0), w_1) = (\phi, w_1), \\ (p'(0), w_2) = (\psi, w_2), \\ (T(0), w_3) = (T_0, w_3), \end{cases} \tag{10}$$

for all $w_1, w_2, w_3 \in L^2(\Omega)$. In equations (8) and (9), $(\cdot,\cdot)$ and $(\cdot,\cdot)_{[L^2]^2}$ are the usual inner products in $L^2(\Omega)$ and $[L^2(\Omega)]^2$, respectively. To simplify the notation, we define

$$Q_p(x,t) = Q(p^2(x,t), (p')^2(x,t), \langle p^2 \rangle (x,t), \langle (p')^2 \rangle (x,t)) \tag{11}$$

as a shorthand notation for the heat source term. Therefore, the piecewise linear finite element (FE) approximations $\hat{p}_H(t) = P_H p_H(t)$ and $\hat{T}_H(t) = P_H T_H(t)$, with $p_H(t), T_H(t) \in V_{H,0}$, are defined by

$$\begin{aligned} (\hat{p}''_H(t), w_{H,1}) + \alpha_1(\hat{p}'_H(t), w_{H,1}) + \alpha_2(\nabla \hat{p}_H(t), \nabla w_{H,1})_{[L^2]^2} + \alpha_3(\nabla \hat{p}'_H(t), \nabla w_{H,1})_{[L^2]^2} \\ = K((\hat{p}_H^2)'', w_{H,1}) + (f(t), w_{H,1}), \end{aligned} \tag{12}$$

$$(\hat{T}'_H(t), w_{H,2}) + \gamma_1(\hat{T}_H(t), w_{H,2}) + \gamma_2(\nabla \hat{T}_H(t), \nabla w_{H,2})_{[L^2]^2} = (Q_{\hat{p}_H(t)}, w_{H,2}) + (g(t), w_{H,2}), \tag{13}$$

a.e. in $(0,t_f)$, for all $w_{H,1}, w_{H,2} \in V_{H,0}$ and

$$\begin{cases} (\hat{p}_H(0), w_{H,1}) = (\hat{\phi}_H, w_{H,1}), \\ (\hat{p}'_H(0), w_{H,2}) = (\hat{\psi}_H, w_{H,2}), \\ (\hat{T}(0), w_{H,3}) = (\hat{T}_{0,H}, w_{H,3}), \end{cases} \tag{14}$$

for all $w_{H,1}, w_{H,2}, w_{H,3} \in V_{H,0}$, with $\hat{\psi}_H = P_H R_H \psi$, $\hat{\phi}_H = P_H R_H \phi$ and $\hat{T}_{0,H} = P_H R_H T_0$. Considering now suitable quadrature rules, from the set of equations (12) to (14) we obtain the fully discrete FE approximations for the acoustic pressure, $p_H(t) \in V_{H,0}$, and for the temperature, $T_H(t) \in V_{H,0}$, that satisfy

$$\begin{aligned} (p''_H(t), w_{H,1})_H + \alpha_1(p'_H(t), w_{H,1})_H + \alpha_2(\nabla_H p_H(t), \nabla_H w_{H,1})_+ \\ +\alpha_3(\nabla_H p'_H(t), \nabla_H w_{H,1})_+ = K\big((p_H^2(t))'', w_{H,1}\big)_H + \Big(\widehat{R}_H f(t), w_{H,1}\Big)_H, \end{aligned} \tag{15}$$

$$\begin{aligned} (T'_H(t), w_{H,2})_H + \gamma_1(T_H(t), w_{H,2})_H + \gamma_2(\nabla_H T_H(t), \nabla_H w_{H,2})_+ \\ = (Q_{\hat{p}_H}(t), w_{H,2})_H + \Big(\widehat{R}_H g(t), w_{H,2}\Big)_H, \end{aligned} \tag{16}$$

a.e. in $(0,t_f)$, for all $w_{H,1}, w_{H,2} \in V_{H,0}$ and

$$\begin{cases} (p_H(0), w_{H,1})_H = (\phi_H, w_{H,1})_H, \\ (p'_H(0), w_{H,2})_H = (\psi_H, w_{H,2})_H, \\ (T_H(0), w_{H,3})_H = (T_H^0, w_{H,3})_H, \end{cases} \tag{17}$$

for all $w_{H,1}, w_{H,2}, w_{H,3} \in V_{H,0}$, where ψ_H, ϕ_H and $T_{0,H}$ are approximations for ψ, ϕ and T_0, respectively. We observe that from equations (15) to (17) we obtain the following initial boundary value problem

$$p''_H(t) + \alpha_1 p'_H(t) = \alpha_2 \Delta_H p_H(t) + \alpha_3 \Delta_H p'_H(t) + K(p_H^2(t))'' + \widehat{R}_H f(t), \tag{18}$$

$$T'_H(t) + \gamma_1 T_H(t) = \gamma_2 \Delta_H T_H(t) + Q_{p_H}(t) + \widehat{R}_H g(t), \tag{19}$$

in Ω_H and a.e. in $(0,t_f)$,

$$p'_H(0) = \psi_H,\ p_H(0) = \phi_H, T_H(0) = T_{0,H}, \text{ in } \overline{\Omega}_H, \tag{20}$$

and

$$p_H(t) = T_H(t) = 0, \text{ on } \partial\Omega_H, \tag{21}$$

a.e. in $(0,t_f)$.

Remark 2. Oftentimes, as mentioned in the Iintroduction, the temperature equation in bioheat transfer models includes the convection term $-\nabla \cdot (\mathbf{v}(p, \nabla p)T)$. In this study, we have chosen to omit this convection term from our numerical analysis to simplify the presentation, but will make remarks on how to handle this term in the main analysis. This decision is based on the observation that, in many practical scenarios, the convection effect is relatively minor compared to the diffusion component of the equation. By excluding this term, we simplify the main analysis while still capturing the essential dynamics of the temperature distribution within the tissue.

To consider a fully discrete in time FEM/FDM, given $S \in \mathbb{N}$, we introduce the following uniform partition on the time interval $[0, t_f]$,

$$\{t_n = n\Delta t, n = 0, \ldots, S\}, \text{with} \Delta t = \frac{t_f}{S}.$$

We also introduce the finite difference operators,

$$D_{-t}u_H^n = \frac{u_H^n - u_H^{n-1}}{\Delta t}, \quad D_{2,t}u_H^n = \frac{D_{-t}u_H^{n+1} - D_{-t}u_H^n}{\Delta t}, \quad D_{c,t}u_H^n = \frac{u_H^{n+1} - u_H^{n-1}}{2\Delta t},$$

for values of n that make the expressions valid. To discretize the time integrals in equation (11), we introduce the first order approximation

$$\langle u_H \rangle^n = \frac{\Delta t}{t_n} \sum_{i=1}^{n} u_H^i, \; n \geq 1,$$

and the corresponding discretization of the heat source term Q_p,

$$Q_{p_H}^n = Q((p_H^n)^2, (D_{-t}p_H^n)^2, \langle p_H^2 \rangle^n, \langle (D_{-t}p_H)^2 \rangle^n), \; n \geq 1.$$

Several approaches can be considered in the time integration of the initial boundary value problem defined by equations (18) to (21). The four-level numerical method we propose considers the following time discretization

$$D_{2,t}p_H^n + \alpha_1 D_{-t}p_H^n = \alpha_2 \Delta_H p_H^{n+1} + \alpha_3 \Delta_H D_{-t}p_H^{n+1} + K D_{2,t}(p_H^{n-1})^2 + \widehat{R}_H f(t_{n+1}), \tag{22}$$

$$D_{-t}T_H^{n+1} + \gamma_1 T_H^{n+1} = \gamma_2 \Delta_H T_H^{n+1} + Q_{p_H}^{n+1} + \widehat{R}_H g(t_{n+1}), \tag{23}$$

in Ω_H, for $n = 1, \ldots, S-1$,

$$D_{-t}p_H^1 = \psi_H, \; p_H^0 = \phi_H, T_H^0 = T_{0,H} \text{ in } \Omega_H, \tag{24}$$

and

$$p_H^n = T_H^n = 0 \text{ in } \partial\Omega_H, \text{ for } n = 1, \ldots, S. \tag{25}$$

Remark 3. In the presence of the convection term, $\nabla \cdot (\mathbf{v}(p, \nabla p)T)$, in the temperature equation, we propose to discretize it as

$$\nabla_{c,H} \cdot (\mathbf{v}(p_H^{n+1}, D_H p_H^{n+1}) T_H^n).$$

This approach treats the convection term semi-implicitly, which maintains stability while keeping the computational cost manageable.

3.1. **Stability analysis for the semidiscrete approximation.** We start by studying the stability of $p_H(t)$, that satisfies equation (18) with $K = 0$, that is,

$$p_H''(t) + \alpha_1 p_H'(t) = \alpha_2 \Delta_H p_H(t) + \alpha_3 \Delta_H p_H'(t) + \widehat{R}_H f(t), \tag{26}$$

a.e. $(0, t_f)$, with homogeneous Dirichlet boundary conditions on $\partial\Omega_H$, or, equivalently,

$$\begin{aligned} (p_H''(t), w_{H,1})_H + \alpha_1 (p_H'(t), w_{H,1})_H + \alpha_2 (\nabla_H p_H(t), \nabla_H w_{H,1})_+ + \alpha_3 (\nabla_H p_H'(t), \nabla_H w_{H,1})_+ \\ = \left(\widehat{R}_H f(t), w_{H,1}\right)_H, \; \forall w_{H,1} \in V_{H,0}, \end{aligned} \tag{27}$$

a.e. $(0, t_f)$.

We now define the following set of assumptions:

H1. *The source functions f and g belong to $H^1(0, t_f; L^2(\Omega))$.*

H2. *For $i = 1, 2$, v_i is a Lipschitz function with constant L_v such that $v_i(0, \mathbf{0}) = 0$.*

H3. *Q is a Lipschitz function with constant L_Q.*

H4. *For all sequence of grids $\{\overline{\Omega}_H\}_H$, $H \in \Lambda$, there exists a positive constant C_{qu} such that*

$$\frac{H_{\max}}{H_{\min}} \leq C_{qu}, \; H \in \Lambda.$$

Remark 4. A brief comment on the previous assumptions. Assumption H4 is a standard condition related to grids/triangulations and is the definition of *quasi-uniformity* of a grid. Assumptions H2 and H3 simply requires the convection and heat source terms to be Lipschitz continuous. We also note that assumption H2 allows linear growth in the variables.

As the coupled system of equations (19) to (21) and (26) is nonlinear, to study stability, we assume that ϕ_H, ψ_H and T_H^0 are perturbed. Let $\tilde{\phi}_H, \tilde{\psi}_H$ and $\tilde{T}_H^0$ denote the corresponding perturbations and let

$$\omega_p(t) = p_H(t) - \tilde{p}_H(t),\ \omega_T(t) = T_H(t) - \tilde{T}_H(t),$$

where $\tilde{p}_H(t)$ and $\tilde{T}_H(t)$ are the solutions of equations (19) and (26) with homogeneous Dirichlet boundary conditions corresponding to the perturbations.

We start by showing a principle of conservation of energy for the acoustic pressure.

Proposition 8. *Assume that assumption H1 holds. Let $p_H \in H^1(0,t_f;V_{H,0}) \cap H^2(0,t_f;V_H)$ denote a solution of equation (26). Then*

$$\|p_H'(t)\|_H^2 + \alpha_3\|\nabla_H p_H(t)\|_+^2 + 2\int_0^t \left(\alpha_1\|p_H'(s)\|_H^2 + \alpha_3\|\nabla_H p_H'(s)\|_+^2\right) \mathrm{d}s$$
$$= \|\psi_H\|_H^2 + \alpha_3\|\nabla_H \phi_H\|_+^2,$$

for all $t \in [0,t_f]$.

Proof. Take $f = 0$ and $w_{H,1} = p_H'(t)$ in equation (27). It can be shown that

$$\frac{1}{2}\frac{\mathrm{d}}{\mathrm{d}t}\left(\|p_H'(t)\|_H^2 + \alpha_2\|\nabla_H p_H(t)\|_+^2\right) + \alpha_1\|p_H'(t)\|_H^2 + \alpha_3\|\nabla_H p_H'(t)\|_+^2 = 0,$$

a. e. $(0,t_f)$. Integrating over $[0,t]$ concludes the proof. □

Remark 5. Under the same regularity conditions as in Proposition 8, and noting that equation (26) is linear in $p_H(t)$, we can apply Proposition 8 to $\omega_p(t)$ to obtain

$$\|\omega_p'(t)\|_H^2 + \alpha_2\|\nabla_H \omega_p(t)\|_+^2 + 2\int_0^t \left(\alpha_1\|\omega_p'(s)\|_H^2 + \alpha_3\|\nabla_H \omega_p'(s)\|_+^2\right) \mathrm{d}s$$
$$= \|\psi_H - \tilde{\psi}_H\|_H^2 + \alpha_3\|\nabla_H(\phi_H - \tilde{\phi}_H)\|_+^2,$$

for all $t \in [0,t_f]$.

As far as $\omega_T(t)$, we can proceed similarly with the caveat of the nonlinearity introduced by the heat source and (possible) convective terms. We start by proving two preliminary results with respect to the estimation of the perturbations associated with the heat source and the convective term.

Proposition 9. *Let $p_H, \tilde{p}_H \in H^2(0,t_f;V_H) \cap H^1(0,t_f;V_{H,0})$ and $w_H \in V_{H,0}$. If assumption H3 holds then*

$$\left|(Q_{p_H}(t) - Q_{\tilde{p}_H}(t), w_H)_H\right| \le 2L_Q\left(\sum_{k=0,1}\left(\max_{t\in[0,t_f]}\left(\|\omega_p^{(k)}\|_{H,\infty}(2\|p_H^{(k)}\|_{H,\infty} + \|\omega_p^{(k)}\|_{H,\infty})\right)\right)\right)\|w_H\|_H,$$

a.e. in $(0,t_f)$.

Proof. Applying the Lipschitz assumption H3 to $(Q_{p_H}(t) - Q_{\tilde{p}_H}(t), w_H)_H$ we easily derive

$$\left|(Q_{p_H}(t) - Q_{\tilde{p}_H}(t), w_H)_H\right| \le L_Q \sum_{(x_i,y_j)\in\overline{\Omega}_H} |\square_{i,j}|(\tau(x_i,y_j,t;p_H,\tilde{p}_H) + \tau(x_i,y_j,t;p_H',\tilde{p}_H'))|w_H(x_i,y_j)|,$$

where

$$\tau(x_i,y_j,t;u_H,\tilde{u}_H) = \left|u_H^2(x_i,y_j,t) - \tilde{u}_H^2(x_i,y_j,t)\right| + \left|\left\langle u_H^2\right\rangle(x_i,y_j,t) - \left\langle \tilde{u}_H^2\right\rangle(x_i,y_j,t)\right|,$$

for $u_H \in H^1(0,t_f;V_{H,0})$. We conclude the proof noting that

$$\tau(x_i,y_j,t;u_H,\tilde{u}_H) \le 2\max_{t\in[0,t_f]}(\|u_H - \tilde{u}_H\|_{H,\infty}(2\|u_H\|_{H,\infty} + \|u_H - \tilde{u}_H\|_{H,\infty})).$$

□

Proposition 10. *Let $p_H, \tilde{p}_H, T_H, \tilde{T}_H v_H \in V_{H,0}$, $\omega_p = p_H - \tilde{p}_H$ and $\omega_T = T_H - \tilde{T}_H$. If assumptions H2 and H4 hold then*

$$\left|\left(M_H(T_H\mathbf{v}(p_H, D_H p_H) - \tilde{T}_H\mathbf{v}(\tilde{p}_H, D_H\tilde{p}_H)), \nabla_H v_H\right)_+\right|$$
$$\le 2L_v\sqrt{3}\left(2\|T_H\|_{H,\infty}\sqrt{\|\omega_p\|_H^2 + (1+C_{qu}^3)\|\nabla_H\omega_p\|_+^2} + 3\|\tilde{p}_H\|_{1,H,\infty}\|\omega_T\|_H\right)\|\nabla_H v_H\|_+,$$

where $\mathbf{v} = (v_1, v_2)$ and $\tilde{v}_i = v_i(\tilde{p}_H, D_H\tilde{p}_H)$, $i = 1, 2$.

Proof. Let $v_i = v_i(p_H, D_H p_H)$ and $\tilde{v}_i = v_i(\tilde{p}_H, D_H \tilde{p}_H)$, $i = 1, 2$. Since

$$\begin{aligned}&(M_H(T_H \mathbf{v}(p_H, D_H p_H) - \tilde{T}_H \mathbf{v}(\tilde{p}_H, D_H \tilde{p}_H)), \nabla_H v_H)_+ \\ &\leq \|M_h(T_H v_1 - \tilde{T}_H \tilde{v}_1)\|_{x,+} \|D_{-x} v_H\|_{x,+} + \|M_k(T_H v_2 - \tilde{T}_H \tilde{v}_2)\|_{y,+} \|D_{-y} v_H\|_{y,+},\end{aligned} \tag{28}$$

we just need to estimate the norms on the right-hand side of inequality (28). The first term can be bound as

$$\begin{aligned}\|M_h(T_H v_1 - \tilde{T}_H \tilde{v}_1)\|_{x,+} &\leq \|T_H(v_1 - \tilde{v}_1)\|_H + \|\omega_T \tilde{v}_1\|_H \\ &\leq \|T_H\|_{H,\infty} \|v_1 - \tilde{v}_1\|_H + \|\omega_T \tilde{v}_1\|_H\end{aligned} \tag{29}$$

while the term involving M_k is estimated similarly.

Using assumptions H2 and H4 it follows from straightforward arguments that

$$\begin{aligned}\|v_1(p_H, D_H p_H) - v_1(\tilde{p}_H, D_H \tilde{p}_H)\|_H^2 &\leq 3L_v^2 \big(\|\omega_p\|_H^2 + \|D_h \omega_p\|_H^2 + \|D_k \omega_p\|_H^2\big) \\ &\leq 3L_v^2 \big(\|\omega_p\|_H^2 + (1 + C_{qu}^3) \|\nabla_H \omega_p\|_+^2\big).\end{aligned} \tag{30}$$

Finally, combining inequalities (28) to (30) and noting that

$$\|\omega_T \tilde{v}_i\|_H \leq 3\sqrt{3}\, M_v \|\tilde{p}_H\|_{1,H,\infty} \|\omega_T\|_H,$$

for $i = 1, 2$, we conclude the proof. □

To simplify the notation, we define

$$\theta_p = \left(\sum_{k=0,1} \left(\max_{t \in [0,t_f]} \Big(\|\omega_p^{(k)}(t)\|_{H,\infty} \Big(2\|p_H^{(k)}(t)\|_H + \|\omega_p^{(k)}(t)\|_{H,\infty} \Big) \Big) \right) \right)^2.$$

Proposition 11. *Under the hypotheses of Proposition 9 and assumption H1, if $T_H, \tilde{T}_H \in H^1(0, t_f; V_H) \cap L^2(0, t_f; V_{H,0})$, then*

$$\|\omega_T(t)\|_H^2 + \int_0^t \|\nabla_H \omega_T(s)\|_{1,H}^2 \, \mathrm{d}s \lesssim \|\omega_T(0)\|_H^2 + \theta_p,$$

for all $t \in [0, t_f]$.

Proof. We start by noting that, for $\omega_T(t) = T_H(t) - \tilde{T}_H(t)$ in equation (16),

$$(\omega_T'(t), \omega_T(t))_H + \gamma_1 \|\omega_T(t)\|_H^2 + \gamma_2 \|\nabla_H \omega_T(t)\|_+^2 = (Q_{p_H}(t)) - Q_{\tilde{p}_H}(t), \omega_T(t))_H,$$

a.e. in $(0, t_f)$. Using Proposition 9, it follows that, for all $\epsilon \neq 0$,

$$\frac{1}{2} \frac{\mathrm{d}}{\mathrm{d}t} \|\omega_T(t)\|_H^2 + (\gamma_1 - 2\epsilon^2) \|\omega_T(t)\|_H^2 + \gamma_2 \|\nabla_H \omega_T(t)\|_+^2 \leq \frac{L_Q^2 \theta_p}{\epsilon^2}.$$

a.e. in $(0, t_f)$. Integrating over $[0, t_f]$ leads to the desired result.

□

Remark 6. In the presence of the convective term, we use Proposition 10 to handle the corresponding perturbation. In this case, a similar inequality as the stability result of Proposition 11 still holds, with the right-hand side replaced by

$$e^{C_T \int_0^t \left(\|\omega_p(s)\|_{1,H,\infty}^2 + \|p_H(s)\|_{1,H,\infty}^2\right) \mathrm{d}s} \left(\|\omega_T(0)\|_H^2 + \int_0^t \big(\|T_H(s)\|_{H,\infty}^2 \|\omega_p(s)\|_{H,\infty}^2 + \theta_p \big) \, \mathrm{d}s \right),$$

where C_T is a positive constant independent of H and t.

We can now conclude a first stability result for the solution of equations (19) and (26) with homogeneous Dirichlet boundary conditions in the sense presented in the following result.

Theorem 1. *Let $p_H, \tilde{p}_H \in H^2(0, t_f; V_H) \cap H^1(0, t_f; V_{H,0})$ and $T_H, \tilde{T}_H \in H^1(0, t_f; V_H) \cap L^2(0, t_f; V_{H,0})$. Under assumptions H1, H3 and H4, for all positive ϵ, there exists a positive $\delta \lesssim H_{\max}$ such that for all solutions of equations* (19) *to* (21) *and* (26) *with* $\max(\|\omega_T(0)\|_H, \|\omega_p'(0)\|_H, \|\omega_p(0)\|_{1,H}) < \delta$, *it holds that*

$$\|\omega_p'(t)\|_H^2 + \|\nabla_H \omega_p(t)\|_+^2 + \int_0^t \|\omega_p'(s)\|_{1,H}^2 \, \mathrm{d}s < \epsilon \tag{31}$$

and

$$\|\omega_T(t)\|_H^2 + \int_0^t \|\omega_T(s)\|_+^2 \, \mathrm{d}s < \epsilon, \tag{32}$$

for all $t \in [0, t_f]$ and $H \in \Lambda$.

Proof. Applying Propositions 8 and 11, it suffices to assume that $\|\omega_p'(0)\|_H$, $\|\nabla_H\omega_p(0)\|_+$ and $\|\omega_T(0)\|_H$ are bounded by a factor $CH_{\max}$, where $C>0$ is a constant independent of H and t. This implies that left hand side of inequalities (31)and (32) are uniformly bounded with respect to H and t.

For the pressure, the proof is trivial. For the temperature, it remains to uniformly bound θ_p. Applying Proposition 3 and Proposition 8, we derive for $k=0,1$, that

$$\begin{aligned}
\|\omega_p^{(k)}(t)\|_{H,\infty} &\le \frac{1}{H_{\min}}\|\omega_p^{(k)}(t)\|_H \\
&\le \frac{\tilde{C}}{H_{\min}}\left(\|\omega_p'(0)\|_H + \|\nabla_H\omega_p(0)\|_+\right) \\
&\le \frac{2\tilde{C}CH_{\max}}{H_{\min}} \\
&\le 2\tilde{C}CC_{qu},
\end{aligned}$$

for some constants $C,\tilde{C}>0$ independent of H and t. The term $\|p_H(t)\|_{H,\infty}$ can be bound uniformly using the same arguments, which yields a uniform bound for θ_p. □

Remark 7. If the heat source term, Q, depends only on p^2 and $(p')^2$, reworking the upper bound given by Proposition 9, then it can be shown that the radius of the balls, δ, centered in $p_H'(0)$, $p_H(0)$ and $T_H(0)$ in Theorem 1 can be taken independently of $H_{\max}$.

Remark 8. If we consider the convection term in the analysis of Theorem 1, stability in the sense stated in this result, is achieved as long as we can control the approximate pressure and temperature, in the $\|\cdot\|_{H,\infty}$ and $\|\cdot\|_{1,H,\infty}$ norms. Indeed, in this case, the inequality provided by Theorem 1 is still valid as long as we further assume suitable bounds for the initial data and a uniform bound for $\|T_H(t)\|_{H,\infty}$ with respect to $H\in\Lambda$ and $t\in[0,t_f]$. Specifically, under assumptions H2 and H4, then it suffices to require that the radius of the balls centered in $T_H(0)$ and $p_H(0)$ are taken as $\delta\lesssim H_{\max}^2$. The uniform bound for $T_H(t)$ can be derived from the upcoming convergence analysis of the semidiscrete approximations, which is established in Section 3.2.

Remark 9. We note that the local stability result in Theorem 1 is established considering that the radius of the balls centered in $T_H(0)$ and $p_H(0)$ are H-dependent. These results follow the definition of stability introduced in the literature by Sanz-Serna and Lopez-Marcos in [17, 18] which is a natural extension of the nonlinear stability concept due to Keller in [15].

3.2. **Convergence analysis of the semidiscrete approximations.** In this section we establish upper bounds for the semidiscretization errors

$$E_p(t) = R_Hp(t) - p_H(t),\; E_T(t) = R_HT(t) - T_H(t),\; \text{in } \overline{\Omega}_H\times[0,t_f],$$

where p,T are the solutions of equations (8) to (10) (with $K=0$) and $p_H(t),T_H(t)$ are the solutions of equations (19) to (21) and (26), all with homogeneous Dirichlet boundary and initial conditions.

On nonuniform grids, assuming $p(t),p'(t),T(t)\in C^4(\overline{\Omega})$ yields first-order spatial truncation errors in the $\|\cdot\|_{H,\infty}$ norm. We establish second-order estimates applying suitable norms under weaker regularity. This is partially achieved using results from [6] based on the Bramble-Hilbert lemma [2].

Proposition 12. *Assume that assumption H1 holds. Let $p\in H^2(0,t_f;H^2(\Omega))\cap H^1(0,t_f;H^3(\Omega)\cap H_0^1(\Omega))$ and $p_H\in H^2(0,t_f;V_H)\cap H^1(0,t_f;V_{H,0})$ denote the solutions of equation* (8) *(with $K=0$) and equation* (26)*, respectively, all with homogeneous Dirichlet boundary conditions. Then*

$$\begin{aligned}
&\|E_p'(t)\|_H^2 + \|\nabla_HE_p(t)\|_+^2 + \int_0^t \|E_p'(s)\|_{1,H}^2\,\mathrm{d}s \\
&\lesssim \|E_p'(0)\|_H^2 + \|\nabla_HE_p(0)\|_+^2 + H_{\max}^4\sum_{i=1,2}\int_0^t\left(\|p^{(i)}(s)\|_{H^2(\Omega)}^2 + \|p^{(i-1)}(s)\|_{H^3(\Omega)}^2\right)\mathrm{d}s,
\end{aligned} \tag{33}$$

for $t\in[0,t_f]$ and $H\in\Lambda$.

Proof. Considering $w_{H,1}=E_p'(t)$ in equation (27) we deduce

$$\begin{aligned}
&\left(p_H''(t),E_p'(t)\right)_H + \alpha_1\left(p_H'(t),E_p'(t)\right)_H + \alpha_2\left(\nabla_Hp_H(t),\nabla_HE_p'(t)\right)_+ \\
&+\alpha_3\left(\nabla_Hp_H'(t),\nabla_HE_p'(t)\right)_+ = \left(\widehat{R}_Hf(t),E_p'(t)\right)_H,
\end{aligned} \tag{34}$$

a.e. in $(0, t_f)$. The term $\left(\widehat{R}_H f(t), E_p'(t)\right)_H$ admits the representation

$$\begin{aligned}
\left(\widehat{R}_H f(t), E_p'(t)\right)_H = &\left(\widehat{R}_H p''(t) - R_H p''(t), E_p'(t)\right)_H + \left(R_H p''(t), E_p'(t)\right)_H \\
&+ \alpha_1 \left(\widehat{R}_H p'(t) - R_H p'(t), E_p'(t)\right)_H + \alpha_1 \left(R_H p'(t), E_p'(t)\right)_H \\
&- \alpha_2 \left(\widehat{R}_H \Delta p(t), E_p'(t)\right)_H - \alpha_2 \left(\nabla_H R_H p(t), \nabla_H E_p'(t)\right)_+ \\
&- \alpha_3 \left(\widehat{R}_H \Delta p'(t), E_p'(t)\right)_H - \alpha_3 \|\nabla_H R_H p'(t)\|_+ \nabla_H E_p'(t) \\
&+ \alpha_2 \|\nabla_H R_H p(t)\|_+ \nabla_H E_p'(t) + \alpha_3 \left(\nabla_H R_H p'(t), \nabla_H E_p'(t)\right)_+ .
\end{aligned} \tag{35}$$

Considering [6, Lemma 5.1], and under the smoothness assumptions on p, we obtain

$$\left| \left(\widehat{R}_H \Delta p(t), E_p'(t)\right)_H + \alpha_2 \|\nabla_H R_H p(t)\|_+ \nabla_H E_p'(t) \right| \lesssim H_{\max}^2 \|p(t)\|_{H^3(\Omega)} \|\nabla_H E_p'(t)\|_+$$

and

$$\left| \left(\widehat{R}_H \Delta p'(t), E_p'(t)\right)_H + \alpha_2 \left(\nabla_H R_H p'(t), \nabla_H E_p'(t)\right)_+ \right| \lesssim H_{\max}^2 \|p'(t)\|_{H^3(\Omega)} \|\nabla_H E_p'(t)\|_+ .$$

Considering now [6, Lemma 5.7], it follows that

$$\left| \left(\widehat{R}_H p''(t) - R_H p''(t), E_p'(t)\right)_H \right| \lesssim H_{\max}^2 \|p''(t)\|_{H^2(\Omega)} \|\nabla_H E_p'(t)\|_+$$

and

$$\left| \left(\widehat{R}_H p'(t) - R_H p'(t), E_p'(t)\right)_H \right| \lesssim H_{\max}^2 \|p'(t)\|_{H^2(\Omega)} \|\nabla_H E_p'(t)\|_+ .$$

Taking into account these estimates and equations (34) and (35), we get

$$\begin{aligned}
\frac{1}{2} \frac{\mathrm{d}}{\mathrm{d}t} \|E_p'(t)\|_H^2 + \alpha_1 \|E_p'(t)\|_H + \frac{\alpha_2}{2} \frac{\mathrm{d}}{\mathrm{d}t} \|\nabla_H E_p(t)\|_+^2 + (\alpha_3 - 4\epsilon^2) \|\nabla_H E_p'(t)\|_+^2 \\
\lesssim \frac{1}{4\epsilon^2} H_{\max}^4 \sum_{i=1,2} \left(\|p^{(i-1)}(t)\|_{H^3(\Omega)}^2 + \|p^{(i)}(t)\|_{H^2(\Omega)}^2 \right),
\end{aligned}$$

for all $\epsilon \neq 0$, a.e. in $(0, t_f)$. Integrating over $[0, t]$ leads to inequality (33). □

We establish now an error estimate for $E_T(t)$.

Proposition 13. *Let $p \in H^2(0, t_f; H^2(\Omega)) \cap H^1(0, t_f; H^3(\Omega) \cap H_0^1(\Omega))$, $T \in L^2(0, t_f; H^3(\Omega) \cap H_0^1(\Omega)) \cap H^1(0, t_f; H^2(\Omega))$, $p_H \in H^1(0, t_f; V_{H,0}) \cap H^2(0, t_f; V_H)$ and $T_H \in L^2(0, t_f; V_{H,0}) \cap H^1(0, t_f; V_H)$ denote the solutions of equations* (8)*,* (9)*,* (19) *and* (26) *(with $K = 0$). If assumptions H1 and H3 hold and $Q(p^2, (p')^2, \langle p^2 \rangle, \langle (p')^2 \rangle) \in L^2(0, t_f; H^2(\Omega))$, then*

$$\|E_T(t)\|_H^2 + \int_0^t \|\nabla_H E_T(s)\|_{1,H}^2 \,\mathrm{d}s \lesssim \|E_T(0)\|_H^2 + H_{\max}^4 T_r(t), \tag{36}$$

for $t \in [0, t_f], H \in \Lambda$, where

$$T_r(t) = \int_0^t \left(\|T(s)\|_{H^3(\Omega)}^2 + \|T'(s)\|_{H^2(\Omega)}^2 + \|Q_p(s)\|_{H^2(\Omega)}^2 \right) \mathrm{d}s.$$

Proof. First, from [6, Lemma 5.7], we obtain

$$\left| (Q_{p_H}(t), E_T(t))_H - \left(\widehat{R}_H Q_p(t), E_T(t)\right)_H \right| \lesssim H_{\max}^2 \|Q_p(t)\|_{H^2(\Omega)} \|\nabla_H E_T(t)\|_+,$$

provided that $Q_p(t) \in H^2(\Omega)$. Second, we have

$$\begin{aligned}
- (\gamma_2 \nabla_H T_H(t), \nabla_H E_T(t))_+ - \left(\gamma_2 \widehat{R}_H \Delta T(t), E_T(t)\right)_H \\
\leq -\gamma_2 \|\nabla_H E_T(t)\|_+^2 + C_T H_{\max}^2 \|T(t)\|_{H^3(\Omega)} \|\nabla_H E_T(t)\|_+ .
\end{aligned}$$

Following the procedure used to establish inequality (33) and taking into account the previous inequalities, we arrive at the desired result. □

From Propositions 12 and 13 we obtain the following result, proving the quadratic convergence rate of the semidiscrete scheme with respect to space.

Theorem 2. *Let* $p \in H^2(0,t_f;H^2(\Omega)) \cap H^1(0,t_f;H^3(\Omega) \cap H_0^1(\Omega))$*,* $T \in L^2(0,t_f;H^3(\Omega) \cap H_0^1(\Omega)) \cap H^1(0,t_f;H^2(\Omega))$*,* $p_H \in H^1(0,t_f;V_{H,0}) \cap H^2(0,t_f;V_H)$ *and* $T_H \in L^2(0,t_f;V_{H,0}) \cap H^1(0,t_f;V_H)$ *denote the solutions of equations* (8)*,* (9)*,* (19) *and* (26) *(with* $K=0$*). If assumptions H1 and H3 hold,* $Q_p \in L^2(0,t_f;H^2(\Omega))$ *and the initial conditions of equations* (19) *and* (26) *are defined by* $p_H'(0) = R_H p'(0)$*,* $p_H(0) = R_H p(0)$ *and* $T_H(0) = R_H T(0)$*, respectively, then*

$$\|E_p'(t)\|_H^2 + \|\nabla_H E_p(t)\|_+^2 + \int_0^t \|E_p'(s)\|_{1,H}^2 \,\mathrm{d}s \lesssim H_{\max}^4 \int_0^t \Theta_p(s)\,\mathrm{d}s,$$

and

$$\|E_T(t)\|_H^2 + \int_0^t \|\nabla_H E_T(s)\|_{1,H}^2 \,\mathrm{d}s \lesssim H_{\max}^4 T_r(t), \tag{37}$$

for $t \in [0,t_f], H \in \Lambda$*, where*

$$\Theta_p(s) = \sum_{i=1,2} \Big(\|p^{(i)}(s)\|_{H^2(\Omega)}^2 + \|p^{(i-1)}(s)\|_{H^3(\Omega)}^2 \Big)$$

and

$$T_r(t) = \int_0^t \Big(\|T(s)\|_{H^3(\Omega)}^2 + \|T'(s)\|_{H^2(\Omega)}^2 + \|Q_p(s)\|_{H^2(\Omega)}^2 \Big)\,\mathrm{d}s$$

Remark 10. In the presence of the convective term and the additional assumption H2, the right-hand side of inequality (36) is replaced by

$$e^{\,C_T \int_0^t \Psi_p(s)\,\mathrm{d}s} \bigg(\|E_T(0)\|_H^2 + \int_0^t \Big(H_{\max}^4 T_r(s) + \|T(s)\|_{L^\infty(\Omega)}^2 \|E_p(s)\|_{1,H}^2 \Big)\,\mathrm{d}s \bigg),$$

for $t \in [0,t_f]$, $H \in \Lambda$, where C_T is a positive constants independent of H and t,

$$\Psi_p(s) = \|E_p(s)\|_{1,H,\infty}^2 + \|p(s)\|_{L^\infty(\Omega)}^2 + \|\nabla p(s)\|_{[L^\infty(\Omega)]^2}^2$$

and

$$T_r(s) = \|T(s)\|_{H^3(\Omega)}^2 + \|T'(s)\|_{H^2(\Omega)}^2 + \|T(s)\|_{L^\infty(\Omega)}^2 \|p(s)\|_{H^3(\Omega)}^2 + \|Q_p(s)\|_{H^2(\Omega)}^2 + \|\mathbf{v}(s)T(s)\|_{[H^2(\Omega)]^2}^2.$$

In this scenario, inequality (37) also holds true adding to the integrand function on the right-hand side the function

$$\|T(s)\|_{H^3(\Omega)}^2 \Big(1 + \|p(s)\|_{H^3(\Omega)}^2\Big) + \|\mathbf{v}(s)T(s)\|_{[H^2(\Omega)]^2}^2 + \|T'(s)\|_{H^2(\Omega)}^2.$$

Remark 11. Coming back to the stability analysis of Section 3.1, we mentioned that a uniform bound for $\|T_H(t)\|_{H,\infty}$ with respect to $H \in \Lambda$ and $t \in [0,t_f]$ is required to establish the stability of equations (19) and (26) when the convection term is considered. Under the assumptions of Theorem 2, assumption H4 and considering the initial condition $T_H(0) = R_H T(0)$, we can conclude that

$$\begin{aligned} \|T_H(t)\|_{H,\infty} &\le \frac{1}{H_{\min}} \|E_T(t)\|_H + \|T\|_{C([0,t_f];C(\overline{\Omega}))} \\ &\lesssim H_{\max} C_{qu} + \|T\|_{C([0,t_f];C(\overline{\Omega}))} \\ &\lesssim 1. \end{aligned}$$

4. Fully discrete scheme in time and space

We now turn to the analysis of the fully discrete scheme,

$$\begin{cases} D_{2,t} p_H^n + \alpha_1 D_{-t} p_H^{n+1} = \alpha_2 \Delta_H p_H^{n+1} + \alpha_3 \Delta_H D_{-t} p_H^{n+1} + \widehat{R}_H f(t_{n+1}), & (38) \\ D_{-t} T_H^{n+1} + \gamma_1 T_H^{n+1} = \gamma_2 \Delta_H T_H^{n+1} + Q_{pH}^{n+1} + \widehat{R}_H g(t_{n+1}), & (39) \end{cases}$$

in Ω_H, for $n = 1, \dots, S-1$, with initial conditions and boundary data given by equations (24) and (25).

Remark 12. The system of equations (24), (25), (38) and (39) has a unique solution for Δt small enough. This can be shown using standard arguments based on the invertibility of the matrices associated with equation (38) and equation (39).

4.1. **Stability.** Let $p_H, \tilde{p}_H$ and $T_H, \tilde{T}_H$ represent two solutions of the equations (24), (25), (38) and (39) and ψ_H, $\tilde{\psi}_H$, ϕ_H, $\tilde{\phi}_H$, $\chi_H, \tilde{\chi}_H$ their corresponding perturbations of the initial data. We define

$$w_{p,H} = p_H - \tilde{p}_H, \quad w_{T,H} = T_H - \tilde{T}_H.$$

Proposition 14. *If* $\max_{i=1,\dots,S}\{\|p_H^i\|_{H,\infty}, \|D_{-t}p_H^i\|_{H,\infty}\} \lesssim 1$ *then, under assumptions H1 and H3, for all* $\epsilon > 0$*, there exists* $\delta \lesssim H_{\max}$ *such that for all solutions of equations* (24)*,* (25)*,* (38) *and* (39) *with* $\max(\|\psi_H - \tilde{\psi}_H\|_{1,H}, \|\phi_H - \tilde{\phi}_H\|_{1,H}, \|\chi_H - \tilde{\chi}_H\|_H) < \delta$*, it follows that*

$$\|D_{-t}w_{p,H}^n\|_H^2 + \alpha_2\|\nabla_H w_{p,H}^n\|_+^2 + 2\Delta t\sum_{i=2}^n\big(\alpha_1\|D_{-t}w_{p,H}^i\|_H^2 + \alpha_3\|\nabla_H D_{-t}w_{p,H}^i\|_+^2\big) \le \epsilon \tag{40}$$

and

$$\|w_{T,H}^n\|_H^2 + \gamma_1\Delta t\sum_{i=1}^n\|w_{T,H}^i\|_H^2 + 2\gamma_2\Delta t\sum_{i=1}^n\|\nabla_H w_{T,H}^i\|_+^2 \le \epsilon, \tag{41}$$

for all $n = 1, \dots, S$.

Proof. For $n \ge 1$, we have

$$\begin{aligned}\big(D_{2,t}w_{p,H}^n, D_{-t}w_{p,H}^{n+1}\big)_H &+ \alpha_1\Big(D_{-t}w_{p,H}^{n+1}, D_{-t}w_{p,H}^{n+1}\Big)_H\\ &+ \alpha_2\Big(\nabla_H w_{p,H}^{n+1}, \nabla_H D_{-t}w_{p,H}^{n+1}\Big)_+ + \alpha_3\Big(\nabla_H D_{-t}w_{p,H}^{n+1}, \nabla_H D_{-t}w_{p,H}^{n+1}\Big)_+ = 0,\end{aligned}$$

which leads to

$$\begin{aligned}(1+2\alpha_1\Delta t)\|D_{-t}w_{p,H}^{n+1}\|_H^2 + \alpha_2\|\nabla_H w_{p,H}^{n+1}\|_+^2 + 2\alpha_3\Delta t\|\nabla_H D_{-t}w_{p,H}^{n+1}\|_+^2\\ \le \|D_{-t}w_{p,H}^n\|_H^2 + \alpha_2\|\nabla_H w_{p,H}^n\|_+^2.\end{aligned}$$

It follows that, for $n \ge 1$,

$$\begin{aligned}\|D_{-t}w_{p,H}^n\|_H^2 + \alpha_2\|\nabla_H w_{p,H}^n\|_+^2 + 2\Delta t\sum_{i=2}^n\big(\alpha_1\|D_{-t}w_{p,H}^i\|_H^2 + \alpha_3\|\nabla_H D_{-t}w_{p,H}^i\|_+^2\big)\\ \le \|\psi_H - \tilde{\psi}_H\|_H^2 + \alpha_2\Delta t^2\|\nabla_H(\psi_H - \tilde{\psi}_H)\|_+^2 + \|\nabla_H(\phi_H - \tilde{\phi}_H)\|_+^2.\end{aligned}$$

yielding inequality (40).

For the temperature, we have

$$\Big(D_{-t}w_{T,H}^{n+1}, w_{T,H}^{n+1}\Big)_H + \gamma_1\|w_{T,H}^{n+1}\|_H^2 + \gamma_2\|\nabla_H w_{T,H}^{n+1}\|_+^2 = \Big(Q_{p_H}^{n+1} - Q_{\tilde{p}_H}^{n+1}, w_{T,H}^{n+1}\Big)_H. \tag{42}$$

Proceeding as in the proof of Proposition 9, it follows that

$$\left|\Big(Q_{p_H}^{n+1} - Q_{\tilde{p}_H}^{n+1}, w_{T,H}^{n+1}\Big)_H\right| \le L_Q M\|w_{T,H}^{n+1}\|_H,$$

where

$$\begin{aligned}M = \max_{n=1,\dots,S}\big(&\|w_{p,H}^n\|_{H,\infty}\big(2\|p_H^n\|_{H,\infty} + \|w_{p,H}^n\|_{H,\infty}\big)\\ &+\|D_{-t}w_{p,H}^n\|_{H,\infty}\big(2\|D_{-t}p_H^n\|_{H,\infty} + \|D_{-t}w_{p,H}^n\|_{H,\infty}\big)\big).\end{aligned}$$

Combining the previous inequality with equation (42) and applying Young's inequality, we obtain for all $\epsilon > 0$,

$$\frac{1}{2}D_{-t}\|u_H^{n+1}\|_H^2 + (\gamma_1 - \epsilon^2)\|u_H^{n+1}\|_H^2 + \gamma_2\|\nabla_H u_H^{n+1}\|_+^2 \le \frac{(L_Q M)^2}{4\epsilon^2}. \tag{43}$$

Choosing $\epsilon^2 = \frac{\gamma_1}{2}$, we derive that, for $n \ge 1$,

$$\|u_H^n\|_H^2 + \gamma_1\Delta t\sum_{i=1}^n\|u_H^i\|_H^2 + 2\gamma_2\Delta t\sum_{i=1}^n\|\nabla_H u_H^i\|_+^2 \le \|u_H^0\|_H^2 + 2(L_Q M)^2 t_n.$$

The proof concludes noticing that $u_H^0 = \chi_H - \tilde{\chi}_H$ and choosing $\delta = CH_{\max}$ sufficiently small such that M is also small, leading to inequality (41). ☐

Remark 13. Proposition 14 shows that the fully discrete scheme defined by equations (24), (25), (38) and (39) is stable with respect to perturbations in the initial data as long as the discrete acoustic pressure and its time derivative, p_H and $D_{-t}p_H$, remain uniformly bounded in the norm $\|\cdot\|_{H,\infty}$. This can be done using the same ideas as presented in Remark 11, the convergence result Proposition 16 and assuming $\Delta t \lesssim H_{\max}$.

Remark 14. In the presence of the convective term and the additional assumption H2, the stability result of Proposition 14 also holds true. The extra term arising from the convection can be controlled as follows (proved similarly to Proposition 9):

$$\begin{aligned}\Big|\big(M_H(T^n_H\mathbf{v}(p^{n+1}_H, D_H p^{n+1}_H) - \tilde{T}^n_H\mathbf{v}(\tilde{p}^{n+1}_H, D_H\tilde{p}^{n+1}_H)), \nabla_H u^{n+1}_H\big)_+\Big| \\ \le \Big(2\sqrt{3}\,L_v\|T^n_H\|_{H,\infty}\sqrt{\|w^{n+1}_{p,H}\|^2_H + (1+C^3_{qu})\|\nabla_H w^{n+1}_{p,H}\|^2_+} \\ +6\sqrt{3}\,M_v\|\tilde{p}^n_H\|_{1,H,\infty}\|w^n_{T,H}\|_H\Big)\|\nabla_H w^{n+1}_{T,H}\|_+.\end{aligned}$$

This upper bound modifies inequality (43) by adding to the right-hand side a term of the form

$$\frac{C_T(\delta)}{2\gamma_2}\left(1+\|w^n_{T,H}\|^2_H\right) + \frac{\gamma_2}{2}\|\nabla_H w^{n+1}_{T,H}\|^2_+,$$

for some positive constant $C_T(\delta)$ satisfying $\lim_{\delta\to 0^+} C_T(\delta) = 0$, provided that $\|w^n_{T,H}\|_H$ and $\|\tilde{p}^n_H\|_{1,H,\infty}$ are uniformly bounded. Thus, we derive

$$D_{-t}\|w^{n+1}_{T,H}\|^2_H + \gamma_1\|w^{n+1}_{T,H}\|^2_H + \gamma_2\|\nabla_H w^{n+1}_{T,H}\|^2_+ \le \frac{C_T(\delta)}{\gamma_2}\left(1+\|w^n_{T,H}\|^2_H\right) + \frac{(L_Q M)^2}{\gamma_1}.$$

Finally, this leads to a stability result similar to inequality (41) but with an exponential growth in time, i.e., for $n\ge 1$,

$$\|w^n_{T,H}\|^2_H + \frac{\gamma_2\Delta t}{1+\gamma_1\Delta t}\sum_{i=1}^n \rho^{n-i}\|\nabla_H w^i_{T,H}\|^2_+ \lesssim e^{\lambda t_n}\|w^0_{T,H}\|^2_H + \frac{M^2 t_n}{1+\gamma_2\Delta t},$$

where $\rho = \frac{1+\frac{C_T(\delta)}{\gamma_2}}{1+\gamma_1\Delta t}$ and $\lambda = \frac{\frac{C_T(\delta)}{\gamma_2}-\gamma_1}{1+\gamma_2\Delta t}$.

4.2. **Convergence.** In this section we will study the convergence of the system of equations (24), (25), (38) and (39). We start by analyzing the acoustic pressure equation. Let us define the following functional space:

$$X_p = C^1([0,t_f]; H^3(\Omega)\cap C^2(\overline{\Omega})\cap H^1_0(\Omega)) \cap C^2([0,t_f]; H^3(\Omega)) \cap H^3(0,t_f; C(\overline{\Omega})).$$

Proposition 15. *Let $p\in X_p$ and $p^n_H \in V_{H,0}$ denote the solutions of equations* (8), (9), (24), (25) *and* (38) *(with $K=0$), respectively. Let $E^n_{p,H}(x_i,y_j) = R_H p(x_i,y_j,t_n) - p^n_H(x_i,y_j)$, $\phi_H(x_i,y_j) = R_H\phi(x_i,y_j)$ and $\psi_H(x_i,y_j) = R_H\psi(x_i,y_j)$, for $i=1,\dots,N$, $j=1,\dots,M$, $n=1,\dots,S$. If assumption H1 holds then*

$$\begin{aligned}&\frac{1}{2}D_{-t}\Big[\|D_{-t}E^{n+1}_{p,H}\|^2_H + \alpha_2\|\nabla_H E^{n+1}_{p,H}\|^2_+\Big] + (\alpha_1-\epsilon_a)\|D_{-t}E^{n+1}_{p,H}\|^2_H + (\alpha_3-\epsilon_b)\|\nabla_H D_{-t}E^{n+1}_{p,H}\|^2_+ \\ &\lesssim H^4_{\max}\Big(\|p'(t_{n+1})\|^2_{H^3(\Omega)} + \|p(t_{n+1})\|^2_{H^3(\Omega)} + \|p''(t_{n+1})\|^2_{H^2(\Omega)}\Big) + \Delta t\Big(\int_{t^{n-1}}^{t_{n+1}}\|R_H p'''(t)\|^2_H \\ &\quad + \|R_H p''(t)\|^2_H + H^2_{\max}\left(\|p''_x(t)\|^2_{L^2(\Omega)} + \|p''_y(t)\|^2_{L^2(\Omega)} + \|p''_{yx}(t)\|^2_{L^2(\Omega)} + \|p''_{xy}(t)\|^2_{L^2(\Omega)}\right)\mathrm{d}t\Big).\end{aligned}$$

for any $\epsilon_a,\epsilon_b>0$.

Proof. The convergence analysis will essentially make use of Bramble-Hilbert lemma [2] and of two lemmas that can be found in [6]. From equation (38), we can write

$$\begin{aligned}\Big(D_{2,t}p^n_H, D_{-t}E^{n+1}_{p,H}\Big)_H + \alpha_1\Big(D_{-t}p^{n+1}_H, D_{-t}E^{n+1}_{p,H}\Big)_H + \alpha_2\Big(\nabla_H p^{n+1}_H, \nabla_H D_{-t}E^{n+1}_{p,H}\Big)_+ \\ +\alpha_3\Big(\nabla_H D_{-t}p^{n+1}_H, \nabla_H D_{-t}E^{n+1}_{p,H}\Big)_+ = \Big(\widehat{R}_H f(t_{n+1}), D_{-t}E^{n+1}_{p,H}\Big)_H.\end{aligned}\tag{44}$$

We note that the right-hand side of equation (44) can be rewritten as

$$\begin{aligned}\Big(\widehat{R}_H f(t_{n+1}), D_{-t}E^{n+1}_{p,H}\Big)_H = \Big(\widehat{R}_H p''(t_{n+1}), D_{-t}E^{n+1}_{p,H}\Big)_H + \alpha_1\Big(\widehat{R}_H p'(t_{n+1}), D_{-t}E^{n+1}_{p,H}\Big)_H \\ - \alpha_2\Big(\widehat{R}_H\Delta p(t_{n+1}), D_{-t}E^{n+1}_{p,H}\Big)_H - \alpha_3\Big(\widehat{R}_H\Delta p'(t_{n+1}), D_{-t}E^{n+1}_{p,H}\Big)_H.\end{aligned}$$

Combining the previous equations leads to

$$\begin{aligned}&\frac{1}{2}D_{-t}\Big[\|D_{-t}E^{n+1}_{p,H}\|^2_H + \alpha_2\|\nabla_H E^{n+1}_{p,H}\|^2_+\Big] + \alpha_1\|D_{-t}E^{n+1}_{p,H}\|^2_H + \alpha_3\|\nabla_H D_{-t}E^{n+1}_{p,H}\|^2_+ \\ &\le \tau_0 + \alpha_1\tau_1 + \alpha_2\tau_2 + \alpha_3\tau_3,\end{aligned}\tag{45}$$

where

$$
\begin{aligned}
\tau_0 &= \Big(D_{2,t} R_H p(t_n) - \widehat{R}_H p''(t_{n+1}), D_{-t} E_{p,H}^{n+1}\Big)_H,\\
\tau_1 &= \Big(D_{-t} R_H p(t_{n+1}) - \widehat{R}_H p'(t_{n+1}), D_{-t} E_{p,H}^{n+1}\Big)_H,\\
\tau_2 &= \Big(\nabla_H R_H p(t_{n+1}), \nabla_H D_{-t} E_{p,H}^{n+1}\Big)_+ + \Big(\widehat{R}_H \Delta p(t_{n+1}), D_{-t} E_{p,H}^{n+1}\Big)_H,\\
\tau_3 &= \Big(\nabla_H D_{-t} p(t_{n+1}), \nabla_H D_{-t} E_{p,H}^{n+1}\Big)_+ + \Big(\widehat{R}_H \Delta p'(t_{n+1}), D_{-t} E_{p,H}^{n+1}\Big)_H.
\end{aligned}
$$

We will now estimate each term τ_i, $i = 0, 1, 2, 3$. In the following, all constants denoted by $C_{i,j}$ and C_k are positive and independent of Δt, n and $H_{\max}$.

- Estimate for τ_0:
  Adding and subtracting suitable terms, τ_0 can be rewritten as

$$
\begin{aligned}
&\underbrace{\Big(D_{2,t} R_H p(t_n) - R_H p''(t_n), D_{-t} E_{p,H}^{n+1}\Big)_H}_{\tau_{0,1}} + \underbrace{\Big(R_H p''(t_n) - R_H p''(t_{n+1}), D_{-t} E_{p,H}^{n+1}\Big)_H}_{\tau_{0,2}}\\
&\qquad + \underbrace{\Big(R_H p''(t_{n+1}) - \widehat{R}_H p''(t_{n+1}), D_{-t} E_{p,H}^{n+1}\Big)_H}_{\tau_{0,3}}.
\end{aligned} \tag{46}
$$

  We will now prove an upper bound for the first term in equation (46), $\tau_{0,1}$. Defining the functional $\ell_0 : W^{3,1}(0,1) \longrightarrow \mathbb{R}$ as $\ell_0(v) = v''(1/2) - v(1) + 2v(1/2) - v(0)$, and considering $v(s) = p(t_n + (2s-1)\Delta t)$, for $s \in [0,1]$, the Bramble-Hilbert lemma [2] implies that

$$
|\tau_{0,1}| \lesssim \left(\Delta t \int_{t^{n-1}}^{t_{n+1}} \|R_H p'''(t)\|_H^2 \,\mathrm{d}t\right)^{1/2} \|D_{-t} E_{p,H}^{n+1}\|_H. \tag{47}
$$

  The second term, $\tau_{0,2}$, can be estimated as

$$
|\tau_{0,2}| \leq \left(\Delta t \int_{t_n}^{t_{n+1}} \|R_H p'''(t)\|_H^2 \,\mathrm{d}t\right)^{1/2} \|D_{-t} E_{p,H}^{n+1}\|_H, \tag{48}
$$

  while the third term, $\tau_{0,3}$, can be estimated using [6, Lemma 5.7], leading to

$$
|\tau_{0,3}| \leq C_{0,3} H_{\max}^2 \, \|p''(t_{n+1})\|_{H^2(\Omega)} \, \|\nabla_H D_{-t} E_{p,H}^{n+1}\|_+. \tag{49}
$$

  Therefore, combining inequalities (47) to (49) and Proposition 2, we obtain

$$
|\tau_0| \lesssim \left(H_{\max}^2 \, \|p''(t_{n+1})\|_{H^2(\Omega)} + \Delta t^{1/2} \left(\int_{t^{n-1}}^{t_{n+1}} \|R_H p'''(t)\|_H^2 \,\mathrm{d}t\right)^{1/2}\right) \|\nabla_H D_{-t} E_{p,H}^{n+1}\|_+. \tag{50}
$$

- Estimate for τ_1:
  For τ_1, writing

$$
\tau_1 = \Big(D_{-t} R_H p(t_{n+1}) - R_H p'(t_{n+1}), D_{-t} E_{p,H}^{n+1}\Big)_H + \Big(R_H p'(t_{n+1}) - \widehat{R}_H p'(t_{n+1}), D_{-t} E_{p,H}^{n+1}\Big)_H,
$$

  we can proceed as for inequalities (47)and (49) and estimate each term separately. This leads to

$$
|\tau_1| \lesssim \left(H_{\max}^2 \, \|p'(t_{n+1})\|_{H^2(\Omega)} + \Delta t^{1/2} \left(\int_{t^{n-1}}^{t_{n+1}} \|R_H p''(t)\|_H^2 \,\mathrm{d}t\right)^{1/2}\right) \|\nabla_H D_{-t} E_{p,H}^{n+1}\|_+. \tag{51}
$$

- Estimate for τ_2:
  Using [6, Lemma 5.1], we obtain the following estimate for τ_2:

$$
|\tau_2| \lesssim H_{\max}^2 \, \|p(t_{n+1})\|_{H^3(\Omega)} \, \|\nabla_H D_{-t} E_{p,H}^{n+1}\|_+.
$$

- Estimate for τ_3:
  We start by writing τ_3 as

$$
\begin{aligned}
\tau_3 &= \Big(\nabla_H R_H p'(t_{n+1}), \nabla_H D_{-t} E_{p,H}^{n+1}\Big)_+ + \Big(\widehat{R}_H \Delta p'(t_{n+1}), D_{-t} E_{p,H}^{n+1}\Big)_H\\
&\quad + \Big(\nabla_H D_{-t} R_H p(t_{n+1}) - \nabla_H R_H p'(t_{n+1}), \nabla_H D_{-t} E_{p,H}^{n+1}\Big)_+.
\end{aligned} \tag{52}
$$

The first two terms in inequality (52) can be estimated using again [6, Lemma 5.1], leading to

$$\begin{aligned}\left|\left(\widehat{R}_H \Delta p'(t_{n+1}), D_{-t}E_{p,H}^{n+1}\right)_H - \left(\nabla_H R_H p'(t_{n+1}), \nabla_H D_{-t}E_{p,H}^{n+1}\right)_+\right|& \\ \lesssim H_{\max}^2 \, \|p'(t_{n+1})\|_{H^3(\Omega)} \, \|D_{-t}E_{p,H}^{n+1}\|_H&.\end{aligned}$$

The second term in inequality (52) can be rewritten as $A_1 + A_2$, where

$$\begin{aligned}A_1 &= \left(D_{-x}\big(R_H p'(t_{n+1}) - D_{-t}R_H p(t_{n+1})\big), D_{-x}D_{-t}E_{p,H}^{n+1}\right)_{x,+} \\ &= \sum_{i=1}^{N}\sum_{j=1}^{M-1} k_{j+1/2}\int_{x_{i-1}}^{x_i} \big(p'_x(x,y_j,t_{n+1}) - D_{-t}p_x(x,y_j,t_{n+1})\big)\,\mathrm{d}x\, D_{-x}D_{-t}E_{p,H}^{n+1}(x_i,y_j),\end{aligned}$$

and

$$\begin{aligned}A_2 &= \left(D_{-y}\big(R_H p'(t_{n+1}) - D_{-t}R_H p(t_{n+1})\big), D_{-y}D_{-t}E_{p,H}^{n+1}\right)_{y,+} \\ &= \sum_{i=1}^{N-1}\sum_{j=1}^{M} h_{i+1/2}\int_{y_{j-1}}^{y_j} \big(p'_y(x_i,y,t_{n+1}) - D_{-t}p_y(x_i,y,t_{n+1})\big)\,\mathrm{d}y\, D_{-y}D_{-t}E_{p,H}^{n+1}(x_i,y_j).\end{aligned}$$

Defining

$$g(x,y,t) = p'_x(x,y,t) - D_{-t}p_x(x,y,t),$$

we can further write

$$\begin{aligned}A_1 = &\underbrace{\sum_{i=1}^{N}\sum_{j=1}^{M-1} k_{j+1/2}\int_{x_{i-1}}^{x_i}\left(g(x,y_j,t_{n+1}) - \frac{1}{k_{j+1/2}}\int_{y_{j-1/2}}^{y_{j+1/2}} g(x,\tau,t_{n+1})\ \mathrm{d}\tau\right)\mathrm{d}x\, D_{-x}D_{-t}E_{p,H}^{n+1}(x_i,y_j)}_{A_{1,1}} \\ &+ \underbrace{\sum_{i=1}^{N}\sum_{j=1}^{M-1}\int_{x_{i-1}}^{x_i}\int_{y_{j-1/2}}^{y_{j+1/2}} g(x,\tau,t_{n+1})\ \mathrm{d}\tau\,\mathrm{d}x\ D_{-x}D_{-t}E_{p,H}^{n+1}(x_i,y_j)}_{A_{1,2}}.\end{aligned} \tag{53}$$

For the first term in inequality (53) we have

$$\begin{aligned}|A_{1,1}| &\le \sum_{i=1}^{N}\sum_{j=1}^{M-1}\int_{x_{i-1}}^{x_i}\int_{y_{j-1/2}}^{y_{j+1/2}}\int_{\tau}^{y_j} |g_y(x,\tau,t_{n+1})|\,\mathrm{d}y\,\mathrm{d}\tau\,\mathrm{d}x\,\left|D_{-x}D_{-t}E_{p,H}^{n+1}(x_i,y_j)\right| \\ &\le \sum_{i=1}^{N}\sum_{j=1}^{M-1} k_{j+1/2}\int_{x_{i-1}}^{x_i}\int_{y_{j-1/2}}^{y_{j+1/2}} |g_y(x,\tau,t_{n+1})|\,\mathrm{d}\tau\,\mathrm{d}x\,\left|D_{-x}D_{-t}E_{p,H}^{n+1}(x_i,y_j)\right|.\end{aligned}$$

We will now use Bramble-Hilbert lemma to estimate $|g_y(x,y,t_{n+1})|$. Consider a functional $\ell : W^{2,1}(0,1) \longrightarrow \mathbb{R}$ defined by $\ell(v) = v'(1) - v(1) + v(0)$, $v \in W^{2,1}(0,1)$. For $\theta(s) = p_{yx}(x,y,t_n + s\Delta t)$, we have $\ell(\theta) = \Delta t g_y(x,y,t_{n+1})$. Applying the Bramble-Hilbert lemma,

$$|\ell(\theta)| \le C_{3,2}\Delta t\int_{t_n}^{t_{n+1}} \left|p''_{yx}(x,y,t)\right|\mathrm{d}t.$$

Therefore, we can estimate $A_{1,1}$ as

$$|A_{1,1}| \lesssim \Delta t^{1/2} H_{\max}\left(\int_{t_n}^{t_{n+1}} \|p''_{yx}(t)\|^2_{L^2(\Omega)}\,\mathrm{d}t\right)^{1/2} \|D_{-x}D_{-t}E_{p,H}^{n+1}\|_{x,+},$$

for all $\mu > 0$.

On the other hand, the last term in inequality (53), $A_{1,2}$, can be estimated using the same tools, leading to

$$|A_{1,2}| \lesssim \Delta t^{1/2} H_{\max}\left(\int_{t_n}^{t_{n+1}} \|p''_{x}(t)\|^2_{L^2(\Omega)}\,\mathrm{d}t\right)^{1/2} \|D_{-x}D_{-t}E_{p,H}^{n+1}\|_{x,+}.$$

Applying the same reasoning to A_2, we obtain

$$|A_1 + A_2| \lesssim \Delta t^{1/2} H_{\max} \left(\int_{t_n}^{t_{n+1}} \|p_x''(t)\|^2_{L^2(\Omega)} + \|p_y''(t)\|^2_{L^2(\Omega)} \,\mathrm{d}t + \int_{t_n}^{t_{n+1}} \|p_{yx}''(t)\|^2_{L^2(\Omega)} + \|p_{xy}''(t)\|^2_{L^2(\Omega)} \,\mathrm{d}t \right)^{1/2} \|\nabla_H D_{-t} E^{n+1}_{p,H}\|_+,$$

giving the final estimate for τ_3,

$$|\tau_3| \lesssim H^2_{\max} \|p'(t_{n+1})\|_{H^3(\Omega)} \|D_{-t} E^{n+1}_{p,H}\|_H + \Delta t^{1/2} H_{\max} \left(\int_{t_n}^{t_{n+1}} \|p_x''(t)\|^2_{L^2(\Omega)} + \|p_y''(t)\|^2_{L^2(\Omega)} \,\mathrm{d}t + \int_{t_n}^{t_{n+1}} \|p_{yx}''(t)\|^2_{L^2(\Omega)} + \|p_{xy}''(t)\|^2_{L^2(\Omega)} \,\mathrm{d}t \right)^{1/2} \|\nabla_H D_{-t} E^{n+1}_{p,H}\|_+. \tag{54}$$

Finally, combining the inequalities (45), (50), (51)and (54), we conclude the proof. □

To provide a complete convergence result for the pressure, we just need estimates for the initial errors $\|D_{-t} E^1_{p,H}\|_H$ and $\|\nabla_H E^1_{p,H}\|_+$. We summarize the previous analysis in the following result.

Proposition 16. *Under the assumptions of Proposition 15, the error for the pressure satisfies*

$$\|D_{-t} E^n_{p,H}\|_H + \|\nabla_H E^n_{p,H}\|_+ + \left(\Delta t \sum_{i=2}^{n} \big(\|D_{-t} E^i_{p,H}\|^2_H + \|\nabla_H D_{-t} E^i_{p,H}\|^2_+ \big) \right)^{1/2} \lesssim H^2_{\max} + \Delta t. \tag{55}$$

Proof. From the inequality of Proposition 15, we obtain

$$\begin{aligned} &\|D_{-t} E^n_{p,H}\|^2_H + \|\nabla_H E^n_{p,H}\|^2_+ + \Delta t \sum_{i=2}^{n} \big(\|D_{-t} E^i_{p,H}\|^2_H + \|\nabla_H D_{-t} E^i_{p,H}\|^2_+ \big) \\ &\lesssim \|D_{-t} E^1_{p,H}\|^2_H + \|\nabla_H E^1_{p,H}\|^2_+ + H^4_{\max} \|p\|^2_{C^2([0,t_f];H^3(\Omega))} \\ &+ \Delta t^2 \int_0^T \Big(\|p\|^2_{H^3(0,t_f;C(\overline{\Omega}))} + H^2_{\max} \|p\|^2_{H^2(0,t_f;H^2(\Omega))} \Big) \,\mathrm{d}t. \end{aligned} \tag{56}$$

The bounds for the initial data $\|D_{-t} E^1_{p,H}\|_H$ and $\|\nabla_H E^1_{p,H}\|_+$ can be derived as in the proof of [7, Theorem 3]:

$$\|D_{-t} E^1_{p,H}\|^2_H \leq \frac{\Delta t^2}{2} \|p\|^2_{C^2([0,t_f];C(\overline{\Omega}))} \tag{57}$$

and

$$\|\nabla_H E^1_{p,H}\|^2_+ \lesssim \Delta t^2 \Big(\Delta t^2 \|p\|^2_{C^2([0,t_f];C^1(\overline{\Omega}))} + H^2_{\max} \|p\|^2_{C^1([0,t_f];C^2(\overline{\Omega}))} \Big). \tag{58}$$

Combining inequalities (56) to (58) we obtain

$$\begin{aligned} &\|D_{-t} E^n_{p,H}\|^2_H + \|\nabla_H E^n_{p,H}\|^2_+ + \Delta t \sum_{i=2}^{n} \big(\|D_{-t} E^i_{p,H}\|^2_H + \|\nabla_H D_{-t} E^i_{p,H}\|^2_+ \big) \\ &\lesssim H^4_{\max} \|p\|^2_{C^2([0,t_f];H^3(\Omega))} + \Delta t^2 \Big(\|p\|^2_{C^2([0,t_f];C(\overline{\Omega}))} + \Delta t^2 \|p\|^2_{C^2([0,t_f];C^1(\overline{\Omega}))} + H^2_{\max} \|p\|^2_{C^1([0,t_f];C^2(\overline{\Omega}))} \\ &+ \int_0^T \Big(\|p\|^2_{H^3(0,t_f;C(\overline{\Omega}))} + H^2_{\max} \|p\|^2_{H^2(0,t_f;H^2(\Omega))} \Big) \,\mathrm{d}t \Big), \end{aligned}$$

which leads to inequality (55). □

We finish this subsection proving an upper bound for the error associated with the heat source term.

Proposition 17. *If $p \in C^2([0,t_f]; C(\overline{\Omega}))$ and $Q_p \in C([0,t_f]; H^2(\Omega))$ then, for all $w_H \in V_{H,0}$,*

$$\begin{aligned} \left| \Big(Q^{n+1}_{p_H} - \widehat{R}_H Q_p(t_{n+1}), w_H \Big)_H \right| &\lesssim H^2_{\max} \|Q_p\|_{C([0,t_f];H^2(\Omega))} \|\nabla_H w_H\|_+ \\ &+ \big(M(E_{p,H}, p) + M(D_{-t} E_{p,H}, p') \big) \|w_H\|_H \\ &+ \Delta t (1 + \Delta t) \|p\|^2_{C^2([0,t_f];C(\overline{\Omega}))} \|w_H\|_H, \end{aligned}$$

where

$$M(u_H, q) = \max_{i=0,\ldots,n} \|u^{i+1}_H\|^2_{L^4_H} + 2 \max_{i=0,\ldots,n} \|u^{i+1}_H\|_H \max_{t \in [0,t_f]} \|R_H q(t)\|_{H,\infty},$$

for $u_H \in V_{H,0}$ and $q \in C([0,t_f]; C(\overline{\Omega}))$.

Proof. We start by decomposing $Q_{p_H}^{n+1} - \widehat{R}_H Q_p(t_{n+1})$ as

$$Q_{p_H}^{n+1} - \widehat{R}_H Q_p(t_{n+1}) = \underbrace{R_H Q_p(t_{n+1}) - \widehat{R}_H Q_p(t_{n+1})}_{S_1} + \underbrace{Q_{p_H}^{n+1} - R_H Q_p^{n+1}}_{S_2} + \underbrace{R_H Q_p^{n+1} - R_H Q_p(t_{n+1})}_{S_3}.$$

We now estimate each term separately. For the first term, S_1, applying the Bramble-Hilbert lemma, we have

$$|(S_1, w_H)_H| \lesssim H_{\max}^2 \, \|Q_p(t_{n+1})\|_{H^2(\Omega)} \, \|\nabla_H w_H\|_+.$$

For the second term, S_2, proceeding similarly as in the proof of Proposition 9, we obtain

$$|(S_2, w_H)_H| \le 2L_Q\big(M(E_{p,H}, p) + M(D_{-t}E_{p,H}, p')\big)\|w_H\|_H.$$

It remains to estimate the term containing S_3. Using the Lipschitz continuity of Q, we obtain for $(x_i, y_j) \in \overline{\Omega}_H$,

$$|S_3(x_i, y_j)| \le L_Q \Bigg(\underbrace{\big|(D_{-t}p(x_i, y_j, t_{n+1}))^2 - (p'(x_i, y_j, t_{n+1}))^2\big|}_{\tau_1}$$
$$+ \underbrace{\left|\big\langle p^2(x_i, y_j, \cdot)\big\rangle^{n+1} - \int_0^{t_{n+1}} p^2(x_i, y_j, t)\,\mathrm{d}t\right|}_{\tau_2} + \underbrace{\left|\big\langle (D_{-t}p(x_i, y_j, \cdot))^2\big\rangle^{n+1} - \int_0^{t_{n+1}} (p')^2(x_i, y_j, t)\,\mathrm{d}t\right|}_{\tau_3} \Bigg)$$

For τ_1, following the proof of Proposition 9 and using the Bramble-Hilbert lemma, we easily obtain

$$\tau_1 \lesssim M\left(\left(\Delta t \int_{t_n}^{t_{n+1}} (R_H p''(t))^2 \,\mathrm{d}t\right)^{1/2}, R_H p'(t_{n+1})\right).$$

The bounds for τ_2 and τ_3 can be derived similarly and accounting for the time integration, leading to

$$\tau_2 \lesssim \frac{1}{t_{n+1}} \sum_{k=1}^{n+1} \int_{t_{k-1}}^{t_k} M\left(\left(\Delta t \int_{t_k}^{t_{k+1}} (R_H p'(s))^2 \,\mathrm{d}s\right)^{1/2}, R_H p(t)\right) \mathrm{d}t$$

and

$$\tau_3 \lesssim \frac{1}{t_{n+1}} \sum_{k=1}^{n+1} \int_{t_{k-1}}^{t_k} M\left(\left(\Delta t \int_{t_k}^{t_{k+1}} (R_H p''(s))^2 \,\mathrm{d}s\right)^{1/2}, R_H p'(t)\right) \mathrm{d}t.$$

Finally, we note that for $u \in C^1([0, t_f]; C(\overline{\Omega}))$, we have

$$M\left(\left(\Delta t \int_{t_n}^{t_{n+1}} (R_H u'(t))^2 \,\mathrm{d}t\right)^{1/2}, R_H u(t_{n+1})\right) \lesssim \Delta t(1 + \Delta t)\, \|u\|^2_{C^1([0,t_f];C(\overline{\Omega}))}$$

and

$$\sum_{k=1}^{n+1} \int_{t_{k-1}}^{t_k} M\left(\left(\Delta t \int_{t_k}^{t_{k+1}} (R_H u'(s))^2 \,\mathrm{d}s\right)^{1/2}, R_H u(t)\right) \mathrm{d}t \lesssim \Delta t(1 + \Delta t)\, \|u\|^2_{C^1([0,t_f];C(\overline{\Omega}))},$$

which leads to

$$|S_3(x_i, y_j)| \lesssim \Delta t(1 + \Delta t)\, \|p\|^2_{C^2([0,t_f];C(\overline{\Omega}))}$$

Combining the previous inequalities concludes the proof. $\square$

Remark 15. Under the assumptions of Proposition 15, the term $M(E_{p,H}, p)$ can be bounded by $C(H_{\max}^2 + \Delta t)^2$, where C is a positive constant independent of $H_{\max}$ and Δt, as well as the first part of $M(D_{-t}E_{p,H}, p')$.

Corollary 1. *If $p \in X_p$, $Q_p \in C([0, t_f]; H^2(\Omega))$, assumption H4 and $\Delta t \lesssim H_{\max}$ then, for all $w_H \in V_{H,0}$,*

$$\left|\left(Q_{p_H}^{n+1} - \widehat{R}_H Q_p(t_{n+1}), w_H\right)_H\right| \lesssim H_{\max}^2 \|\nabla_H w_H\|_+ + (H_{\max}^2 + \Delta t + \Delta t^2)\|w_H\|_H$$

Proof. From Proposition 17, we only need to establish bounds for the terms $M(E_{p,H},p)$ and $M(D_{-t}E_{p,H},p')$. Using the definition of $M(E_{p,H},p)$, Proposition 7 and Proposition 16, we have

$$\begin{aligned}
M(E_{p,H},p) &= \max_{i=0,\dots,n}\|E_{p,H}^{i+1}\|_{L_H^4}^2 + 2\max_{i=0,\dots,n}\|E_{p,H}^{i+1}\|_H \max_{t\in[0,t_f]}\|R_H p(t)\|_{H,\infty}\\
&\le \sqrt{2}\max_{i=0,\dots,n}\|E_{p,H}^{i+1}\|_H\|\nabla_H E_{p,H}^{i+1}\|_+ + 2\max_{i=0,\dots,n}\|E_{p,H}^{i+1}\|_H \max_{t\in[0,t_f]}\|R_H p(t)\|_{H,\infty}\\
&\lesssim H_{\max}^4+\Delta t^2 + (H_{\max}^2+\Delta t)\,\|p\|_{C([0,t_f];C(\overline{\Omega}))}\\
&\lesssim H_{\max}^2+\Delta t+\Delta t^2.
\end{aligned}$$

On the other hand, using Proposition 16, we have

$$M(D_{-t}E_{p,H},p') \lesssim \max_{i=0,\dots,n}\Big(\|D_{-t}E_{p,H}^{i+1}\|_{H,\infty}\|D_{-t}E_{p,H}^{i+1}\|_H\Big) + H_{\max}^2+\Delta t. \tag{59}$$

Applying Proposition 3 to the discrete infinity norm in inequality (59) and using the upper bound from Proposition 16, we obtain

$$\begin{aligned}
M(D_{-t}E_{p,H},p') &\lesssim \frac{1}{H_{\min}}\max_{i=0,\dots,n}\|D_{-t}E_{p,H}^{i+1}\|_H^2 + H_{\max}^2+\Delta t\\
&\lesssim \frac{H_{\max}^4+\Delta t^2}{H_{\min}} + H_{\max}^2+\Delta t.
\end{aligned}$$

From assumption H4 and $\Delta t\lesssim H_{\max}$, we conclude the proof. □

Remark 16. If the heat source term does not depend on the integral of p_t^2, the result from Corollary 1 can be improved since we do not require the restriction on the time step size.

Let us now analyse the convergence of the temperature approximation. Let

$$X_T = C([0,t_f];H^3(\Omega))\cap H^2(0,t_f;C(\overline{\Omega})).$$

We start by stating the following result.

Proposition 18. *Let $p\in X_p$, $p_H^n\in V_{H,0}$, $T\in X_T$ and $T_H^n\in V_{H,0}$ denote the solutions of equations (8) and (10), equations (24) and (38), equations (9) and (10) and equations (24) and (39) respectively. Let $E_{T,H}^n(x_i,y_j)=R_HT(x_i,y_j,t_n)-T_H^n(x_i,y_j)$, for $i=1,\dots,N$, $j=1,\dots,M$ and $n=1,\dots,S$. If $p\in X_p$, $T\in X_T$, $Q_p\in C([0,t_f];H^2(\Omega))$, under assumptions H1, H3 and H4 and $\Delta t\lesssim H_{\max}$ then*

$$\begin{aligned}
&\frac{1}{2}D_{-t}\Big(\|E_{T,H}^{n+1}\|_H^2\Big) + (\gamma_1-\epsilon_a)\Big\|E_{T,H}^{n+1}\Big\|_H^2 + (\gamma_2-\epsilon_b)\Big\|\nabla_H E_{T,H}^{n+1}\Big\|_+^2\\
&\lesssim H_{\max}^4+\Delta t^2 + H_{\max}^4\Big(\|T(t_{n+1})\|_{H^3(\Omega)}^2+\|T'(t_{n+1})\|_{H^2(\Omega)}^2\Big) + \Delta t\int_{t^{n-1}}^{t_{n+1}}\|R_HT''(t)\|_H^2\,\mathrm{d}t,
\end{aligned}\tag{60}$$

for any $\epsilon_a,\epsilon_b>0$.

Proof. We can write

$$\begin{aligned}
&\Big(D_{-t}T_H^{n+1},E_{T,H}^{n+1}\Big)_H + \gamma_2\Big(\nabla_H T_H^{n+1},\nabla_H E_{T,H}^{n+1}\Big)_+ + \gamma_1\Big(T_H^{n+1},E_{T,H}^{n+1}\Big)_H\\
&= \Big(Q_{p_H}^{n+1},E_{T,H}^{n+1}\Big)_H + \Big(\widehat{R}_H g(t_{n+1}),E_{T,H}^{n+1}\Big)_H.
\end{aligned}\tag{61}$$

Proceeding as in the proof of Proposition 15, we can rewrite equation (61) as

$$\begin{aligned}
&\Big(D_{-t}E_{T,H}^{n+1},E_{T,H}^{n+1}\Big)_H + \gamma_1\Big\|E_{T,H}^{n+1}\Big\|_H^2 + \gamma_2\Big\|\nabla_H E_{T,H}^{n+1}\Big\|_+^2 = (D_{-t}R_HT(t_{n+1})-\widehat{R}_HT_t(t_{n+1}),E_{T,H}^{n+1})_H\\
&+\gamma_1\Big(R_HT(t_{n+1})-\widehat{R}_HT(t_{n+1}),E_{T,H}^{n+1}\Big)_H + \Big(\widehat{R}_HQ_{p(t_{n+1})}-Q_{p_H}^{n+1},E_{T,H}^{n+1}\Big)_H\\
&+\gamma_2\bigg(\Big(\widehat{R}_H(\Delta T(t_{n+1})),E_{T,H}^{n+1}\Big)_+ + \Big(\nabla_H R_HT(t_{n+1}),\nabla_H E_{T,H}^{n+1}\Big)_+\bigg).
\end{aligned}\tag{62}$$

Following the proof of Proposition 15, from equation (62) we derive

$$\begin{aligned}
&\frac{1}{2}D_{-t}\Big(\|E_{T,H}^{n+1}\|_H^2\Big) + \gamma_1\Big\|E_{T,H}^{n+1}\Big\|_H^2 + \gamma_2\Big\|\nabla_H E_{T,H}^{n+1}\Big\|_+^2\\
&\lesssim \Big(\widehat{R}_HQ_{p(t_{n+1})}-Q_{p_H}^{n+1},E_{T,H}^{n+1}\Big)_H + H_{\max}^2\,\|T(t_{n+1})\|_{H^3(\Omega)}\,\|\nabla_H E_{T,H}^{n+1}\|_+\\
&+\left(H_{\max}^2\,\|T'(t_{n+1})\|_{H^2(\Omega)} + \Delta t^{1/2}\Big(\int_{t^{n-1}}^{t_{n+1}}\|R_HT''(t)\|_H^2\,\mathrm{d}t\Big)^{1/2}\right)\|\nabla_H D_{-t}E_{T,H}^{n+1}\|_+
\end{aligned}$$

Using Corollary 1 we obtain

$$\begin{aligned}&\frac{1}{2}\,D_{-t}\Big(\|E_{T,H}^{n+1}\|_H^2\Big)+\gamma_1\Big\|E_{T,H}^{n+1}\Big\|_H^2+\gamma_2\Big\|\nabla_H E_{T,H}^{n+1}\Big\|_+^2\\&\lesssim H_{\max}^2\|\nabla_H E_{T,H}^{n+1}\|_+ +(H_{\max}^2+\Delta t)\|E_{T,H}^{n+1}\|_H+H_{\max}^2\,\|T(t_{n+1})\|_{H^3(\Omega)}\,\|\nabla_H E_{T,H}^{n+1}\|_+\\&+\left(H_{\max}^2\,\|T'(t_{n+1})\|_{H^2(\Omega)}+\Delta t^{1/2}\left(\int_{t^{n-1}}^{t_{n+1}}\|R_H T''(t)\|_H^2\,\mathrm{d}t\right)^{1/2}\right)\|\nabla_H D_{-t}E_{T,H}^{n+1}\|_+.\end{aligned}$$

Applying Young's inequality leads to inequality (60). □

We summarize the previous analysis in the following result.

Corollary 2. *Under the assumptions of Proposition 18, the error for the temperature satisfies*

$$\|E_{T,H}^n\|_H+\left(\Delta t\sum_{i=1}^n\big(\|E_{T,H}^i\|_H^2+\|\nabla_H E_{T,H}^i\|_+^2\big)\right)^{1/2}\lesssim H_{\max}^2+\Delta t. \tag{63}$$

Proof. The proof follows the same steps as in Proposition 16. □

Remark 17. If the convective term is present, the convergence analysis remains valid under the additional assumption that $\Delta t\lesssim H_{\max}^2$. Under the same assumptions of Proposition 18, and using the upper bound from Proposition 10, we can prove that

$$\begin{aligned}&\frac{1}{2}\,D_{-t}\Big(\|E_{T,H}^{n+1}\|_H^2\Big)+(\gamma_1-\epsilon_a)\Big\|E_{T,H}^{n+1}\Big\|_H^2+(\gamma_2-\epsilon_b)\Big\|\nabla_H E_{T,H}^{n+1}\Big\|_+^2\\&\lesssim H_{\max}^4+\Delta t^2+H_{\max}^4\Big(\|T(t_{n+1})\|_{H^3(\Omega)}^2+\|T'(t_{n+1})\|_{H^2(\Omega)}^2\Big)+\Delta t\int_{t^{n-1}}^{t_{n+1}}\|R_H T''(t)\|_H^2\,\mathrm{d}t,\\&+\big(\|R_H T(t_n)\|_{H,\infty}(H_{\max}^2+\Delta t)+\|p_H^{n+1}\|_{1,H,\infty}\|E_{T,H}^n\|_H\big)\|\nabla_H E_{T,H}^{n+1}\|_+,\end{aligned} \tag{64}$$

for any $\epsilon_a,\epsilon_b>0$.

Since

$$\|p_H^{n+1}\|_{1,H,\infty}\le\|E_{p,H}^{n+1}\|_{1,H,\infty}+\|R_H p(t_{n+1})\|_{1,H,\infty},$$

using Proposition 3 and Proposition 16, we derive

$$\|p_H^{n+1}\|_{1,H,\infty}\le\frac{H_{\max}^2+\Delta t}{H_{\min}^2}+\|p\|_{C([0,t_f];C^1(\overline{\Omega}))}\,.$$

Since $\Delta t\lesssim H_{\max}^2$, from assumption H4 we conclude that $\|p_H^{n+1}\|_{1,H,\infty}$ is uniformly bounded. Thus, proceeding as in the proof of Corollary 2 the error for the temperature approximation satisfies a bound like inequality (63).

We finally state our main convergence result for the fully discrete scheme.

Theorem 3. *Let $p\in X_p$, $p_H^n\in V_{H,0}$, $T\in X_T$ and $T_H^n\in V_{H,0}$ denote the solutions of equations* (8) *and* (10)*, equations* (24) *and* (38)*, equations* (9) *and* (10) *and equations* (24) *and* (39) *respectively. If $p\in X_p$, $T\in X_T$, $Q_p\in C([0,t_f];H^2(\Omega))$ and under assumptions H1, H3 and H4 then, for $n=1,\ldots,S$,*

$$\begin{aligned}&\|D_{-t}E_{p,H}^n\|_H+\|\nabla_H E_{p,H}^n\|_+ +\|E_{T,H}^n\|_H\\&\quad+\left(\Delta t\sum_{i=1}^n\big(\|E_{T,H}^i\|_H^2+\|\nabla_H E_{T,H}^i\|_+^2+\|D_{-t}E_{p,H}^i\|_H^2+\|\nabla_H D_{-t}E_{p,H}^i\|_+^2\big)\right)^{1/2}\lesssim H_{\max}^2+\Delta t.\end{aligned}$$

5. Numerical Simulation

This section aims at illustrating the robustness of the theoretical results previously proven for the fully discrete scheme as well as a simulation of the ideas behind the numerical scheme presented, applied to the linearized Westervelt–Pennes system of equations (5) and (6). We begin in Section 5.1 by validating the convergence properties of our proposed scheme defined by equations (24), (25), (38) and (39), as established in Theorem 3. Following this, in Section 5.2, we shift our focus to a more complex scenario: the simulation of the coupled Westervelt–Pennes system under realistic parameters. This simulation, although applied to a simplified Westervelt–Pennes problem, remains relevant as it showcases the robustness of our space discretization and illustrates the behavior of this system's solutions. All simulations presented in this section were obtained using the Bramble.jl library [25].

5.1. **Estimated convergence order.** We start by illustrating the convergence results proven in Theorem 3 and show that we have a convergence rate drop if we decrease the regularity of the exact solution of the linearized Westervelt–Pennes problem defined by equations (5) and (6). Let $\Omega = (0,1)^2$ and

$$T(x,t) = p(x,t) = 2(x-1)(y-1)|2y-1|^{\mu},\ x \in \overline{\Omega}, t \in [0,1],$$

where $\mu > 0$. Depending on the choice of the parameter μ, we can control the regularity of p and T. In fact, if $\mu = 2$, both functions are in $C^\infty([0,t_f];H^3(\Omega))$, while if $\mu = 1.6$, they are in $C^\infty([0,t_f];H^2(\Omega))$ but not $C^\infty([0,t_f];H^3(\Omega))$. We choose all parameters $\alpha_1, \alpha_2, \alpha_3, \gamma_1$ and γ_2 to be equal to 1, $Q(u_1,u_2,u_3,u_4) = u_1+u_2+u_3+u_4$ and determine f,g such that p and T are the exact solutions of the differential problem. To simplify the calculations, we purposely choose p and T independent of t. This simplifies the calculation of f,g as well as the regularity requirements with respect to time. We stress that the numerical method still maintains the discretization of the time dependent integrals in the source term of the heat equation, which is a key aspect of our analysis and numerical scheme.

If p_H^n and T_H^n are the numerical approximations for $p(\cdot,t_n)$ and $T(\cdot,t_n)$, respectively, determined by equations (24), (25), (38) and (39), then we define the discrete errors:

$$\mathbb{E}_{p,H}^n = \|D_{-t}E_{p,H}^n\|_H + \|\nabla_H E_{p,H}^n\|_+ + \left(\Delta t \sum_{i=2}^{n} (\|D_{-t}E_{p,H}^i\|_{1,H}^2)\right)^{1/2}$$

and

$$\mathbb{E}_{T,H}^n = \left(\|E_{T,H}^n\|_H^2 + \Delta t \sum_{l=1}^{n} \|E_{T,H}^l\|_{1,H}^2\right)^{1/2},$$

for $n = 0,\dots,N$.

To initialize our simulations, we start with two grids of random points in $[0,1]$ and form a cartesian grid suitable for $\overline{\Omega}$. The cartesian grid is then refined by introducing, in each coordinate grid, the midpoint in each subinterval. The first grid starts with 3 points in the x direction and 4 points in the y direction.

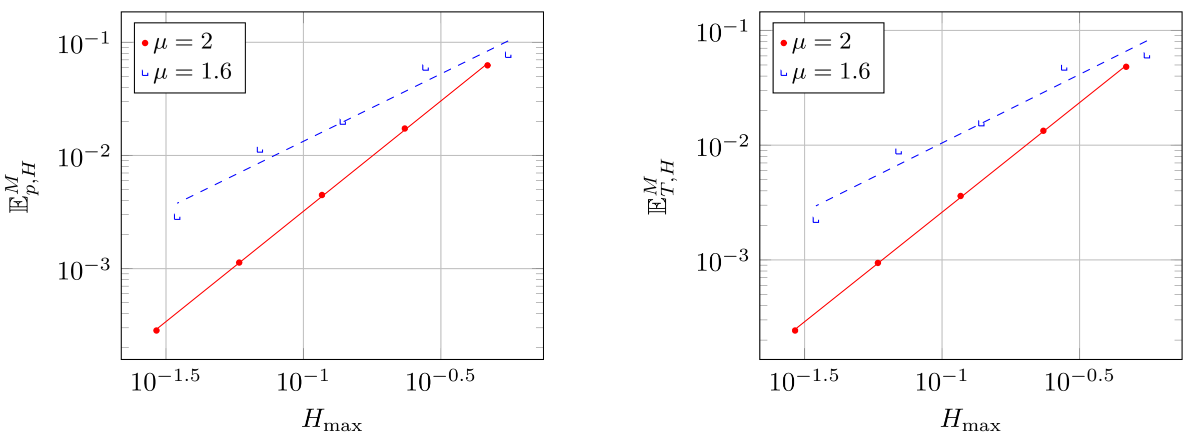

(A) Pressure (B) Temperature

FIGURE 1. Log-log plots of the errors *versus* h_{max}. The lines represent least-squares fittings to the data.

In Figure 1, we plot, using a log-log scale, the previous errors, $\mathbb{E}_{p,H}^M$ and $\mathbb{E}_{T,H}^M$. The average slope of the solid lines, associated with $\mu = 2$, are roughly equal to 1.93, for pressure and temperature. Regarding the average slope associated with the simulation for the less smooth solution ($\mu = 1.6$), it is roughly 1.19. This illustrates an estimated convergence rate close to 2 as shown in Theorem 3 as well as a drop in estimated convergence rate if the solutions (with respect to space) are in H^2 but not H^3.

5.2. **Simulation of HIFU propagation and heating using the Westervelt–Pennes model.** This section details the numerical simulation of HIFU propagation and the associated thermal effects on a biological tissue. The simulation is based on a simplified version of the nonlinear coupled Westervelt–Pennes system of equations (1) to (4) and is inspired on the one documented in [10]. We will use a finite difference approach based on the one defined by equations (22) to (25).

5.2.1. *Computational domain and setup.* We define the 2D computational domain as the rectangle $\Omega = [-4\,\text{cm}, 8\,\text{cm}] \times [-6\,\text{cm}, 6\,\text{cm}]$. The computational domain mainly represents water, except for the region on the rectangle $\Omega_t = [-2.5\,\text{cm}, 2.5\,\text{cm}] \times [-2.25\,\text{cm}, 2.25\,\text{cm}]$ which models a biological tissue with the properties of liver. The circular ultrasound transducer is positioned on the left boundary of the domain ($x = -4\,\text{cm}$). It is focused towards the origin with a focal length of 5 cm and features an aperture angle of 30°. The computational domain, the biological tissue region and the transducer location are illustrated in Figure 2.

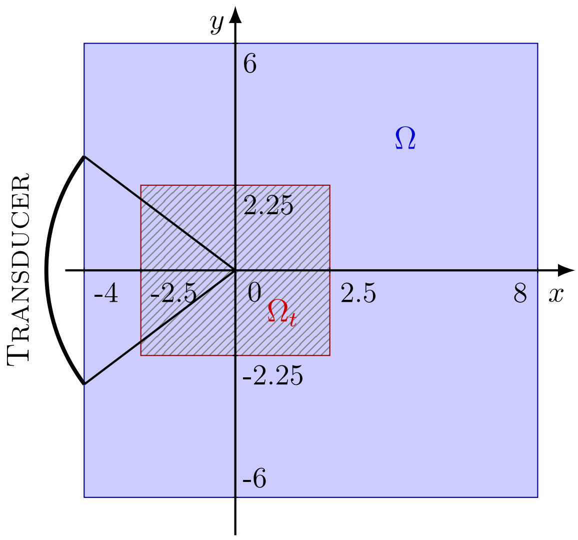

Figure 2. Schematic of the 2D computational domain Ω used for the simulation.

5.2.2. *Simplified Westervelt–Pennes system.* The underlying physical phenomena are modeled by coupling a simplified Westervelt equation for acoustic pressure and the Pennes equation for temperature. The governing Westervelt equation reads as

$$\frac{1}{\rho_m c_m^2}\, p_{tt} = \nabla \cdot \left(\frac{1}{\rho_m}\, \nabla p + \frac{\delta_m}{\rho_m c_m^2}\, \nabla p_t \right) + \frac{\beta_m}{\rho_m^2 c_m^4}\, (p^2)_{tt}, \quad \text{in } \Omega \times (0, t_f] \tag{65}$$

where c_m is the speed of sound, ρ_m is the ambient density, δ_m is the diffusivity of sound, and β_m is the coefficient of nonlinearity of the material. The sound diffusivity is calculated with the formula

$$\delta_m = \frac{2\alpha_m c_m^3}{\omega^2}$$

where $\omega = 2\pi f_0$ is the angular frequency and f_0 is the transducer's emitting frequency.

Symbol	Property	Unit	Water	Liver	Blood
ρ_m	Density	kg/m^3	998.21	1078.75	1060
c_m	Speed of sound	m/s	1482	1586	–
α_m	Attenuation coefficient	Np/m	0.025	6.915	–
β_m	Nonlinear coefficient		3.6	4.4	–
k_m	Thermal conductivity	W/(m °C)	0.6	0.52	–
C_m	Heat capacity	J/(kg °C)	4180	3540	3770
ω_b	Volumetric blood perfusion rate	$\text{kg/(m}^3\,\text{s)}$	0	10	–

Table 1. Physical parameters.

Symbol	Property	Unit	Value
f_0	Frequency	MHz	1.1
a	Radius	cm	2.5
d	Focal length	cm	5
γ	Aperture angle	°	30
p_0	Source pressure magnitude	MPa	0.5

TABLE 2. Parameters for the domain and transducer.

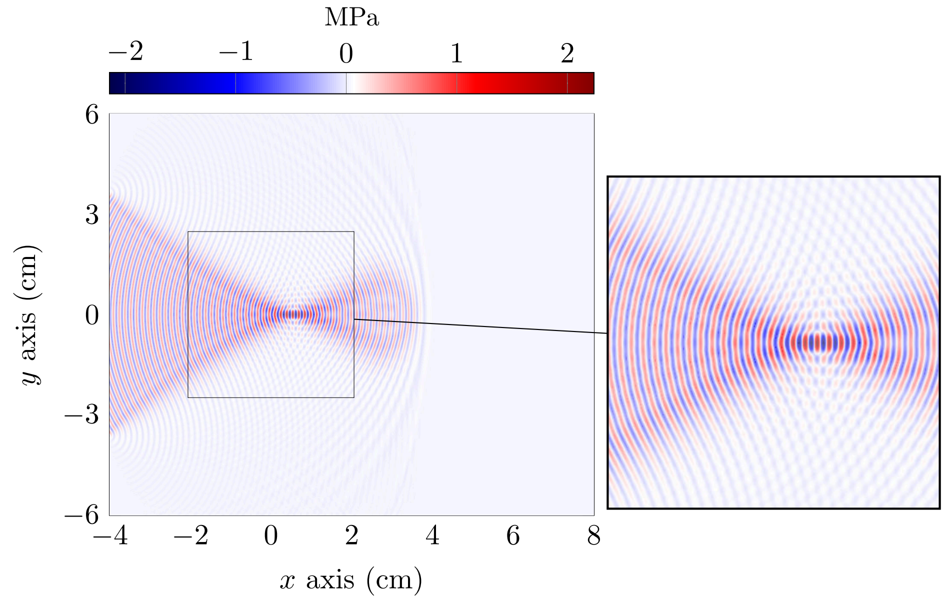

FIGURE 3. Pressure plot on the whole computational domain (left) and a zoom on the target tissue (right).

Remark 18. Note that (65) differs from the pressure equation in (1). Specifically, the speed of sound and nonlinear coefficient are assumed constant, instead of dependent on T. This simplification was adopted due to the lack of data regarding the dependence of the speed of sound with respect to the temperature.

The temperature evolution in the domain, T, is described by the Pennes equation

$$\rho_m C_m \frac{\partial T}{\partial t} = \nabla \cdot (k_m \nabla T) - \omega_b C_b (T - T_{art}) + Q(p), \quad \text{in } \Omega \times (0, t_f] \tag{66}$$

where C_m is the specific heat capacity of the material, k_m is the thermal conductivity, ω_b represents the blood perfusion rate term, C_b is specific heat capacity of blood, $T_{art} = 37\,°\mathrm{C}$ is the arterial blood temperature, and $Q(p)$ is the volumetric heat source generated by the absorption of ultrasound energy. The heat source $Q(p)$ is calculated from the acoustic intensity $I(p)$ and absorption coefficient α_m by $Q(p) = 2\alpha_m I(p)$ where the time-averaged intensity is given by

$$I(p, (x,t)) = \frac{1}{\rho_m c_m t} \int_0^t p^2(x,s)\,\mathrm{d}s\,,\ t > 0. \tag{67}$$

The specific physical parameters used in the simulation are listed in Tables 1 and 2 and have been compiled from [9,10]. These values represent the properties of the simulated biological tissue and water, as well as the characteristics of the ultrasound transducer's source. Throughout this section all parameters with the subscript "$_w$" are relative to water, "$_t$" are relative to the tissue and "$_b$" are relative to blood. Regarding initial and boundary conditions for the pressure field, we impose a Dirichlet boundary condition at $\Gamma = \{(x,y) \in \mathbb{R}^2 : x = -4\}$, derived using planar pressure source approximation [11], given by

$$p(-4,y,t) = \begin{cases} \dfrac{p_0}{\sqrt{1+\frac{y^2}{d^2}}} F\left(t + \frac{d}{c_w}\left(\sqrt{1+\frac{y^2}{d^2}} - 1\right)\right), & y \le d\tan(\gamma) \\ 0, & y > d\tan(\gamma) \end{cases}$$

where $\gamma = \arcsin(\frac{a}{d})$ and $F(t) = \sin(\omega t)$, $t \geq 0$. In the remaining boundary, we use a discretization of the plane wave boundary condition

$$p_t = -c_w \nabla p \cdot \eta, \text{ on } \partial\Omega \backslash \Gamma$$

to avoid spurious reflections on the pressure field. For the temperature field, we consider $T = 37\,°\mathrm{C}$ in $\partial\Omega$. Finally, we take the initial data for the pressure and its velocity as zero and the initial temperature is taken as $37\,°\mathrm{C}$.

5.2.3. *Numerical results.* The fully discrete method used is equations (22) to (25) with the adaptations to account for the coefficients in equations (65) and (66) and the heat source term Q. The plane wave boundary condition is discretized with backward differences in time.

The Westervelt–Pennes system is very challenging to solve due to the nonlinearity present on the pressure equation as well as the typical very oscillatory behavior of the pressure field, under high frequencies. We start by illustrating the effect of the damping and nonlinearity of the Westervelt equation on the acoustic pressure profile versus the standard wave equation. To this end, we plot in Figures 4 and 3 the numerical pressure and intensity at $t_f = 50\,\mu\mathrm{s}$ corresponding to both equations. The discretization parameters for this simulation are $N = 1000$, $M = 600$, $\Delta t = 10\,\mathrm{ns}$ and the mesh is chosen uniform in each direction. We note that this magnitude of the timestep is required to capture the oscillatory behavior of the source term as well as the pressure profile.

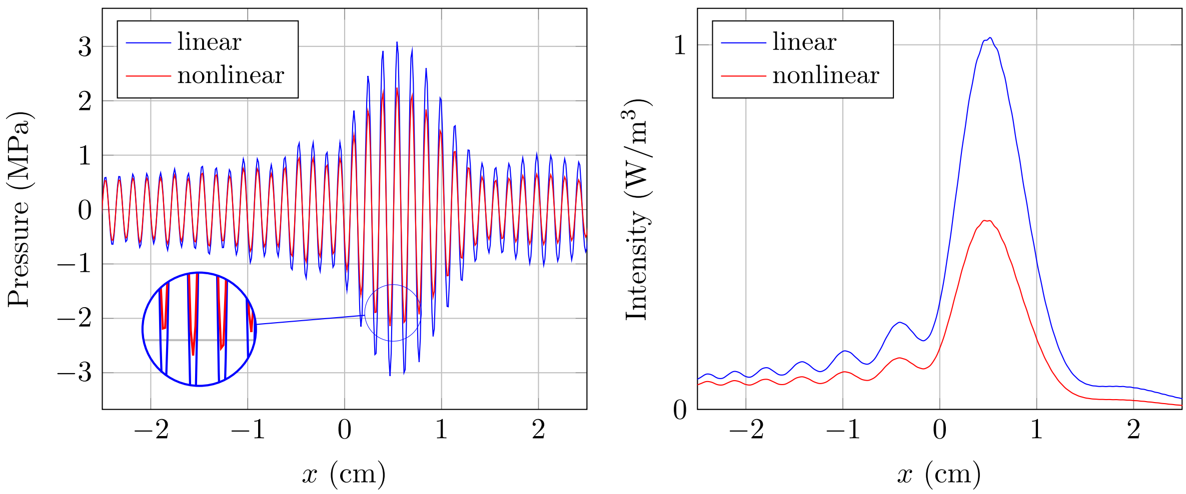

(A) Acoustic pressure.

(B) Intensity.

FIGURE 4. Plots for pressure and intensity at $t = 50\,\mu\mathrm{s}$ along the x axis at $y = 0$ in the target tissue.

To illustrate the behavior of the coupled Westervelt–Pennes system, we now focus on simulating both pressure and temperature for a longer time interval. Due to the oscillatory nature of the solution of the Westervelt equation in the HIFU regime, as mentioned before, a small timestep needs to be employed. However, in our numerical experiments, for the source magnitudes we considered, we noticed that around $T = 300\,\mu\mathrm{s}$ while the pressure still oscillates in time, the pressure intensity (and consequently, the volumetric heat source term Q) stabilizes its variation in time. We then solve the temperature equation only from that point on with that heat source with a timestep $\Delta t = 1\,\mathrm{ms}$. Regarding the space discretization, to also illustrate that our method can employ nonuniform grids, we built a mesh that is more refined in the target tissue. More specifically, if N and M are the number of points to assign to the x and y variables, we create a mesh that is a.e. uniform (in each direction), except for the transition between water and tissue element. Table 3 details the number of points used in each interval, in each direction.

We conducted some simulations with frequency equal to $1.1\,\mathrm{MHz}$ and different magnitudes for the source pressure. In Figure 5 we present the plots for the temperature at $T = 5\,\mathrm{s}$ in Figure 5 for the full computational domain as well as the target tissue. The results illustrate the clear benefits of using HIFU in targeted tissue ablation. While most of the domain remains in an interval of "safe" temperatures, at the focus of the ultrasound we observe a very localized increase in the temperature, in a small time

direction	**subinterval**	**number of points**
x	$[-4\,\mathrm{cm}, -2.5\,\mathrm{cm}]$	$\frac{N}{6}$
	$[-2.5\,\mathrm{cm}, 2.5\,\mathrm{cm}]$	$\frac{7N}{12}$
	$[3\,\mathrm{cm}, -8\,\mathrm{cm}]$	$\frac{N}{4}$
y	$[-6\,\mathrm{cm}, -2.25\,\mathrm{cm}]$	$\frac{M}{6}$
	$[-2.25\,\mathrm{cm}, 2.25\,\mathrm{cm}]$	$\frac{2M}{3}$
	$[2.25\,\mathrm{cm}, 6\,\mathrm{cm}]$	$\frac{M}{6}$

TABLE 3. Number of points to create the mesh for simulating the pressure and temperature of the Westervelt–Pennes system.

window. Increasing the source's magnitude we can have a faster increase in the temperature at the target tissue.

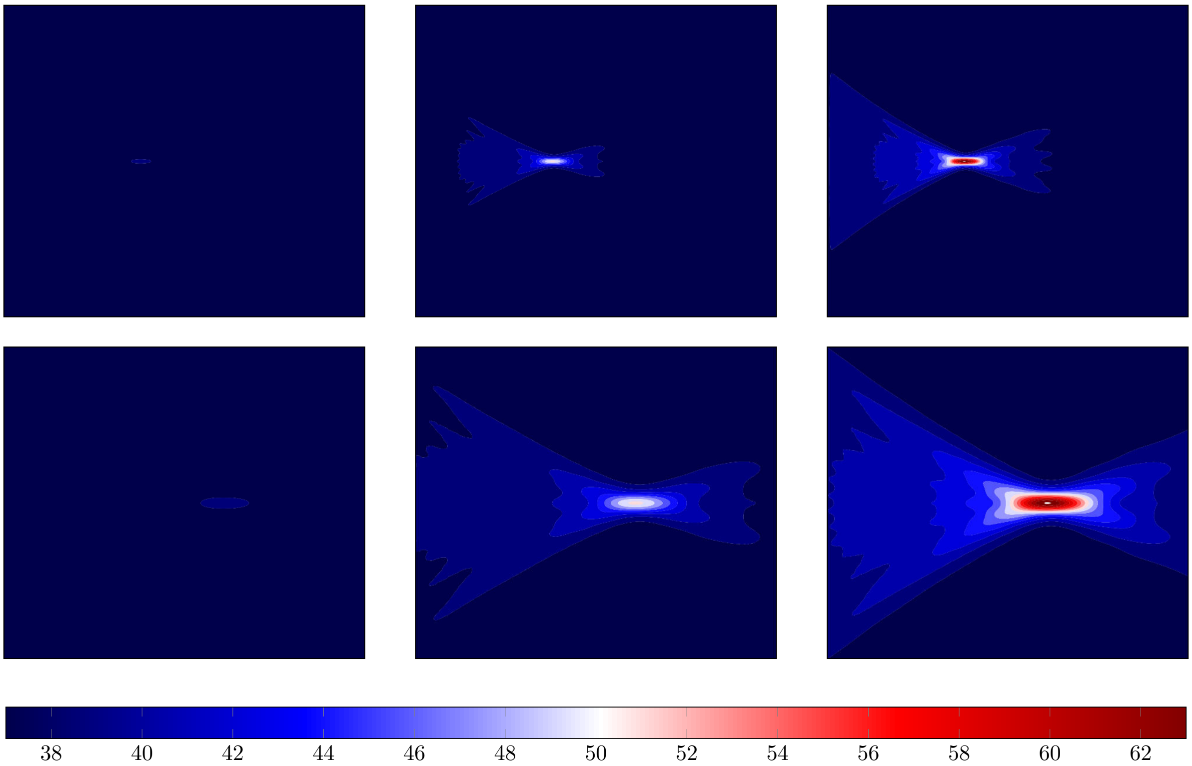

FIGURE 5. Temperature plots in the full domain (top row) and in target tissue (bottom row). The columns correspond to simulations with frequency 1.1 MHz and source pressure magnitude (from left to right) equal to 0.2 MPa, 0.5 MPa and 0.7 MPa.

CONCLUSIONS

In this paper we have presented a numerical method, based on finite differences, to solve the the nonlinear coupled Westervelt–Pennes system. The semidiscrete and fully discrete versions of the method we presented and their stability and convergence properties were analyzed taking into account the linearized version of the Westervelt equation. In particular, we showed second order convergence in space and first order convergence in time for the pressure and temperature fields under standard assumptions on $H_{\max}$ and Δt with and without convective effects acting on the temperature field. This lead to show the stability of the scheme, since it implied that the numerical solution is uniformly bounded in the appropriate norms. We further illustrated the convergence order of in space the fully discrete method, as well as the convergence rate drop when less regular solutions are considered.

We also presented some numerical simulations in a two-dimensional scenario, which show the expected behavior of the pressure and temperature fields. Due to the timescale of the problem, we had to use a very small timestep to capture the oscillatory behavior of the pressure field. A better approach might be to combine the finite difference method proposed in space with a time-stepping method that is adaptative and more suitable for oscillatory problems, such as certain classes of Runge-Kutta methods.

The results also illustrate the benefits of using HIFU for targeted tissue ablation. Future work includes the study of the numerical method applied to the fully nonlinear problem.

Acknowledgment

The authors acknowledge financial support by the Centre for Mathematics of the University of Coimbra (CMUC, https://doi.org/10.54499/UID/00324/2025) under the Portuguese Foundation for Science and Technology (FCT), Grants UID/00324/2025 and UID/PRR/00324/2025. Gonçalo Pena was also financed by national funds from FCT – Fundação para a Ciência e a Tecnologia, I.P., within the context of the project HiPMos4C setting with reference 2023.16854.ICDT2023.16854.ICDT (https://doi.org/10.54499/2023.16854.ICDT).

References

[1] I. Benabbas and B. Said-Houari. The Westervelt-Pennes-Cattaneo model of nonlinear thermo–acoustics: local well-posedness and singular limit for vanishing relaxation time. *SIAM Journal on Mathematical Analysis*, 56:2968–3003, 2024.

[2] J. H. Bramble and S. R. Hilbert. Estimation of linear functionals on Sobolev spaces with application to Fourier transforms and spline interpolation. *SIAM Journal on Numerical Analysis*, 7(1):112–124, 1970.

[3] J. Careaga, V. Nikolić, and B. Said-Houari. Westervelt-based modeling of ultrasound-enhanced drug delivery. *Journal of Nonlinear Science*, 35:61, 2025.

[4] M. Dehbani, M. Rahimi, and Z. Rahimi. A review on convective heat transfer enhancement using ultrasound. *Diagnostic and Interventional Imaging*, 208:118273, 2022.

[5] I. Elhelf, H. Albahar, U. Shah, A. Oto, E. Cressman, and M. Almekkawy. High intensity focused ultrasound: the fundamentals, clinical applications and research trends. *Diagnostic and Interventional Imaging*, 99:349–359, 2018.

[6] J.A. Ferreira and R. Grigorieff. Supraconvergence and supercloseness of a scheme for elliptic equations on non-uniform grids. *Numerical Functional Analysis and Optimization*, 27:539–564, 2006.

[7] J.A. Ferreira, D. Jordão, and L. Pinto. Second order approximations for kinetic and potential energies in maxwell's wave equations. *Applied Numerical Mathematics*, 120:125–140, 2017.

[8] J.A. Ferreira, Daniela Jordão, and L. Pinto. Drug delivery enhanced by ultrasound: mathematical modelling and simulation. *Computers and Mathematics with Applications*, 107:57–69, 2022.

[9] Pragya Gupta and Atul Srivastava. Numerical analysis of thermal response of tissues subjected to high intensity focused ultrasound. *International Journal of Hyperthermia*, 35(1):419—-434, October 2018.

[10] Samaneh Haddadi and Mohammad Taghi Ahmadian. Analysis of nonlinear acoustic wave propagation in HIFU treatment using Westervelt equation. *Scientia Iranica*, pages 2087–2097, September 2017.

[11] Mark F. Hamilton. Comparison of three transient solutions for the axial pressure in a focused sound beam. *The Journal of the Acoustical Society of America*, 92(1):527—-532, July 1992.

[12] W. Huanga, J. Li Y. Jiaob, Y. Hea, W. Shaob, and Y. Cui. Evaluation of dual-frequency switching hifu for optimizing superficial ablation. *Ultrasound in Medicine and Biology*, 50:908–919, 2024.

[13] F. Kashkooli, T. Hornsby, M. Kolios, and J. Tavakkoli. Ultrasound-mediated nano-sized drug delivery systems for cancer treatment: multi-scale and multi-physics computational modeling. *WIREs Nanomedicine and Nanobiotechnology*, e1913, 2023.

[14] F. Kashkooli, A. Jakmola, T. Hornsby, J. Tavakkoli, and M. Kolios. Ultrasound-mediated nano drug delivery for treatment cancer: fundamental physics and future directions. *Journal of Controlled Release*, 355:552–578, 2023.

[15] H. Keller. Approximation methods for nonlinear problems with application to two-point boundary values problems. *Mathematics of Computation*, 29:464–474, 1975.

[16] A. Kyriakou, E. Neufeld, B. Werner, G. Székely, and N. Kuster. Full-wave acoustic and thermal modeling of transcranial ultrasound propagation and investigation of skull-induced aberration correction techniques: a feasibility study. *Journal of Therapeutic Ultrasound*, 3:11, 2015.

[17] J. López-Marcos and J. Sanz-Serna. Stability and convergence in numerical analysis iii: linear investigation of nonlinear stability. *IMA Journal of Numerical Analysis*, 8:71–84, 1988.

[18] J. López-Marcos and J. Sanz-Serna. A definition of stability for nonlinear problems. *Numerical Treatment of Differencial Equations, Proceedings of the Fourth Seminar "NUMDIFF-4", Halle, Edt. K. Strehmel*, Teubner-Texte zur MathematiK, Band 104:216–226, Leipzig 1988.

[19] A. Maio, G. Alfieri, M. Mattone, P. Ghanouni, and A. Napoli. High-intensity focused ultrasound surgery for tumor ablation: a review of current applications. *Radiology: Imaging Cancer*, 6(1):e230074, 2024.

[20] M. Malinen, T. Huttunen, and J. Kaipio. An optimal control approach for ultrasound induced heating. *International Journal of Control*, 76:1323–1336, 2003.

[21] S. Mortazavi and M. Mokhtari-Dizaji. Numerical study of high-intensity focused ultrasound (HIFU) in fat reduction. *Skin Research and Technology*, 2023(29):e13280, 2023.

[22] Vanja Nikolić and Belkacem Said-Houari. Local well-posedness of a coupled Westervelt–Pennes model of nonlinear ultrasonic heating. *Nonlinearity*, 35(11):5749–5780, 2022.

[23] Vanja Nikolić and Belkacem Said-Houari. The Westervelt-Pennes model of nonlinear thermoacoustics: Global solvability and asymptotic behaviour. *Journal of Differential Equations*, 336:628–653, 2022.
[24] Filipa Oliveira. Stability and convergence analysis of a discrete linearised Westervelt–Pennes IBVP, 2024.
[25] Gonçalo Pena. Bramble.jl, 2024. https://github.com/gpena/Bramble.jl.
[26] E. Perolina, S. Meissner, B. Raos, Bruce Harlan, S. Thakur, and D. Svirskis. Translating ultrasound-mediated drug delivery technologies for cns applications. *Advanced Drug Delivery Reviews*, 208:115274, 2024.
[27] Allan D. Pierce. *Acoustics: An Introduction to Its Physical Principles and Applications*. Springer International Publishing, 2019.
[28] S. Poinard, A. Ganeau, M. Lafond, O. Dorado, S. Catheline, C. Lafon, F. Aptel, G. Thuret, and P. Gain. Ultrasound applications in ophthalmology: a review. *Innovation and Research in BioMedical Engineering*, 45:100828, 2024.
[29] A. Pulkkinen, B. Werner, E. Martin, and K. Hynynen. Numerical simulations of clinical focused ultrasound functional neurosurgery. *Physics in Medicine and Biology*, 59:1679–1700, 2014.
[30] Gail ter Haar and Constantin Coussios. High intensity focused ultrasound: Physical principles and devices. *International Journal of Hyperthermia*, 23(2):89–104, 2007.
[31] J. Wang, Z. Li, M. Pan, M. Fiaz, Y. Hao, Y. Yan, and L. Sun. Ultrasound-mediated blood barrier opening: an effective drug delivery system for theranostic of brain diseases. *Advanced Drug Delivery Reviews*, 190:114539, 2022.
[32] T. Wessapan, P. Keangin, P. Rattanadecho, and N. Somsuk. Comparative analysis of heat transfer dynamics in high-intensity focused ultrasound and microwave ablation for cancer treatment. *International Journal of Thermofluids*, 26:101090, 2025.
[33] T. Wessapan and P. Rattanadecho. Flow and heat transfer through a porous tumor during high-intensity focused ultrasound. *International Journal of Heat and Mass Transfer*, 216:124501, 2023.
[34] Peter J. Westervelt. Parametric acoustic array. *The Journal of the Acoustical Society of America*, 35(4):535–537, 04 1963.
[35] C. Yang, J. Jessen, and K. Lin. Ultrasound-assisted ocular drug delivery: a review of current evidence. *Journal of Clinical Ultrasound*, 50:685–693, 2022.

University of Coimbra, CMUC, Department of Mathematics, FCTUC, Largo D. Dinis, 3000–143 Coimbra, Portugal
Email address: ferreira@mat.uc.pt, goncalo.pena@uc.pt, filipaholiveira1@gmail.com